T cells were infected at the acute infection stage but that the infused cells are less infected during chronic infection stage. Alternatively, leaky expression of MazF in the infused MazF-Tmac cells may inhibit the integration of SHIV. Another possibility is that vigorously infected MazF-Tmac cells died off after the over-induction of MazF expression. Further investigation is needed to reveal the mechanism.

We analyzed the function of the MazF-Tmac cells that persisted long after transplantation. Conditional MazF expression system was maintained and MazF protein expressed in T cells harvested from the rhesus macaques long after transplantation. In the freshly isolated samples, which are not expanded *ex vivo*, MazF signal was beyond detection (**Figure 5b**, lane 1). This phenomenon was considered due to low frequency of SHIV infection in MazF-Tmac cells (**Figure 5c**). However, we believe that low sensitivity to SHIV and low expression of MazF may contribute to the stable long-term persistence of MazF-Tmac cells, even in the presence of SHIV. Moreover, our qPCR analysis demonstrated that SHIV replication was blocked (**Figure 5d**). Although these data are from only one macaque, it appears that the MazF expression system was maintained, and the expressed MazF was functional long after transplantation.

Transplantation with MazF-Tmac cells contributed to an increase in the CD4$^+$ T cell counts, and the MazF-Tmac cells showed little or no immunogenicity in rhesus macaques in the presence of SHIV infection, suggesting that the autologous transplantation of MazF-modified CD4$^+$ T cells is an attractive strategy for HIV-1 gene therapy.

Materials and methods

General laboratory statement. Research sample processing and freezing were performed in a biosafety level (BSL) 3 laboratory at the Tsukuba Primate Research Center in the National Institute of Biomedical Innovation (NIBIO, Ibaraki, Japan). Laboratory analyses were performed in BSL2 laboratories at the Tsukuba Primate Research Center in NIBIO and at the Center for Cell and Gene Therapy of Takara Bio, which uses established standard operating procedures and protocols for sample processing, freezing, and analysis.

Study design. The animal study protocol was approved by the Ministry of Education, Culture, Sports, Science and Technology of Japan (identifier 20–8156), and by the Animal Welfare and Animal Care Committee of the NIBIO (identifier DS20-98R3). The study was conducted according to the "Rules for Animal Care and the Guiding Principles for Animal Experiments Using Nonhuman Primates" formulated by the Primate Society of Japan,[33] and in accordance with the recommendations of the Weatherall report, "The use of nonhuman primates in research" and the "Rules for Animal Care and Management of the Tsukuba Primate Research Center."[34] The experimental design is diagrammed in **Figure 1**. Six rhesus macaques, #12, #13, #14, #15, #16, and #17, were used for this experiment. CD4$^+$ T cells were isolated from the blood samples taken from each rhesus macaque before the challenge with SHIV and cryopreserved as described below. After confirming the set point of the SHIV viral loads, the gene-modified CD4$^+$ T cells were manufactured and transplanted as described in **Supplementary Materials**. Autologous CD4$^+$ T cells were transduced with the MazF retroviral vector MT-MFR-PL2 (#12, #13, #14, and #15) or the control vector MT-ZGR-PL2 (#16 and #17).

Animals. The Burmese rhesus macaques were maintained at the Tsukuba Primate Research Center in NIBIO. All surgical and invasive clinical procedures were conducted in a surgical facility using aseptic techniques and comprehensive physiologic monitoring. Ketamine hydrochloride (Ketalar, 10 mg/kg; Daiichi-Sankyo, Tokyo, Japan) was used to induce anesthesia for all clinical procedures associated with the study protocol, including blood sampling, gene-modified cell administration and clinical examinations or treatment.

SHIV 89.6P virus. A CXCR4-tropic SHIV 89.6P[26] was used for this experiment. SHIV 89.6P was propagated in rhesus macaque PBMCs. The culture supernatants were harvested, and the 50% tissue culture infective dose ($TCID_{50}$) was determined by infecting the CD4$^+$ human T-lymphoblastoid cell line M8166 with dilutions of the virus.[35] All the stock viruses were stored at −80°C until use. An intravenous challenge with SHIV 89.6P was performed at 5.0×10^3–1.8×10^5 $TCID_{50}$ (**Supplementary Table S1**).

Gibbon ape leukemia virus (GaLV)-enveloped gamma-retroviral vector MT-MFR-PL2 and MT-ZGR-PL2. The preparation of the retroviral vector used in this study has been previously described.[21] Briefly, an HIV-1-LTR-MazF-polyA cassette was introduced in the direction opposite of the MoMLV-LTR at the multiple cloning site of the retroviral vector plasmid pMT.[36] The *ΔLNGFR* gene[37] was introduced into the retrovirus vector as a surface marker. The *ΔLNGFR* gene is under the control of the human phosphoglycerate kinase (PGK) promoter. The resultant MT-MFR-PL2 was introduced into the packaging cell line PG13 (ATCC CRL-10686) and the GaLV-enveloped gamma-retroviral vector MT-MFR-PL2 was obtained by harvesting the culture fluid of the producer cells. For the control experiment, the *mazF* gene was replaced with the gene encoding the fluorescent ZsGreen1 protein (MT-ZGR-PL2). The GaLV-enveloped MT-ZGR-PL2 was obtained by harvesting the culture fluid of the PG13 derived producer cells.

CD4$^+$ T cells. Prior to the challenge with SHIV 89.6P, the peripheral blood of rhesus macaques was collected by apheresis as described previously.[38] The CD4$^+$ T cells were positively isolated using anti-CD4 antibody conjugated magnetic beads (Dynal CD4 Positive Isolation Kit, Life Technologies, Carlsbad, CA) according to the manufacturer's instructions. The isolated CD4$^+$ T cells were cryopreserved and stored at −80°C until use.

Manufacturing autologous gene-modified CD4$^+$ T cells and transplantation into rhesus macaques. Refer to the **Supplementary Materials**.

Measurement of hematological data. Refer to the **Supplementary Materials.**

Flow cytometry analyses. Refer to the **Supplementary Materials.**

Quantification of gene-modified CD4+ T cells. Refer to the **Supplementary Materials.**

Analyses of the SHIV viral loads in plasma. Refer to the **Supplementary Materials.**

Detection of MazF antigen-specific IFN-γ secreting cells. Refer to the **Supplementary Materials.**

Detection of anti-MazF or anti-ZsGreen1 antibodies in rhesus macaque blood. Refer to the **Supplementary Materials.**

Collection of lymphocytes from several organs. Refer to the **Supplementary Materials.**

Examination of function and antiviral efficacy of persisting MazF-Tmac cells. Refer to the **Supplementary Materials.**

LAM-PCR. Refer to the **Supplementary Materials.**

Western blotting. Refer to the **Supplementary Materials.**

Supplementary material

Figure S1. Body weight and hematological data.
Figure S2. MazF peptides used for the IFN-γ enzyme-linked immunospot assay.
Figure S3. Histopathological analysis of axillary lymph nodes.
Figure S4. Changes in SHIV viral loads, ZsGreen1 proviral copy numbers and production of anti-ZsGreen1 antibodies of rhesus macaque #17.
Figure S5. Linear amplification-mediated (LAM)-PCR.
Table S1. Dose of SHIV 89.6P TCID50 used to infect each rhesus macaque and the time of transplantation of the gene-modified cells.
Table S2. Analysis of the in vivo safety (individual histopathological findings from the autopsy samples).
Materials and methods

Acknowledgments. The authors thank the staff of the Tsukuba Primate Research Center and Corporation for Production and Research of Laboratory Primates for their kind care and expert handling of the animals. The authors thank Keith A. Reimann of Harvard Medical School and Tomoyuki Miura of Kyoto University for providing the SHIV 89.6P. The authors thank the members of the Center for Cell and Gene Therapy of Takara Bio Inc., Koichi Inoue and Katsuyuki Dodo for their contributions and helpful advice, and Hiroshi Tsuda, Tomomi Sakuraba, and Mayumi Shimomura for technical support. The authors have no support or funding to report. The animal study was designed by Hideto Chono, Naoki Saito, Hiroaki Shibata, Naohide Ageyama, Yasuhiro Yasutomi and Junichi Mineno. Gene-modified T cells were manufactured by Naoki Saito and Hideto Chono. All surgical and invasive clinical procedures were conducted under the supervision of Naohide Ageyama. Blood samples were prepared by Hiroaki Shibata. The laboratory analyses were performed by Naoki Saito. The manuscript was written by Hideto Chono and Naoki Saito. All authors discussed and interpreted results. Naoki Saito, Hideto Chono and Junichi Mineno are employees of Takara Bio Inc. (http://www.takara-bio.com). European patent applications EP1921136B1 "Nucleic acid for treatment or prevention of immunodeficiency virus infection" and EP2138580B1 "Vector for gene therapy" were filed through Takara Bio Inc. These interests do not alter the authors' adherence to the Journal's policies regarding sharing data and materials. The other authors declared that they have no competing interests.

1. Kitahata, MM, Gange, SJ, Abraham, AG, Merriman, B, Saag, MS, Justice, AC *et al.* (2009). Effect of early versus deferred antiretroviral therapy for HIV on survival. *N Engl J Med* **360**: 1815–1826.
2. Maartens, G and Boulle, A (2007). CD4 T-cell responses to combination antiretroviral therapy. *Lancet* **370**: 366–368.
3. Geng, EH and Deeks, SG (2009). CD4+ T cell recovery with antiretroviral therapy: more than the sum of the parts. *Clin Infect Dis* **48**: 362–364.
4. Lekakis, J and Ikonomidis, I (2010). Cardiovascular complications of AIDS. *Curr Opin Crit Care* **16**: 408–412.
5. Núñez, M (2010). Clinical syndromes and consequences of antiretroviral-related hepatotoxicity. *Hepatology* **52**: 1143–1155.
6. Cheung, MC, Pantanowitz, L and Dezube, BJ (2005). AIDS-related malignancies: emerging challenges in the era of highly active antiretroviral therapy. *Oncologist* **10**: 412–426.
7. Siliciano, RF and Greene, WC (2011). HIV latency. *Cold Spring Harb Perspect Med* **1**: a007096.
8. Richman, DD, Margolis, DM, Delaney, M, Greene, WC, Hazuda, D and Pomerantz, RJ (2009). The challenge of finding a cure for HIV infection. *Science* **323**: 1304–1307.
9. Hütter, G, Nowak, D, Mossner, M, Ganepola, S, Müssig, A, Allers, K *et al.* (2009). Long-term control of HIV by CCR5 Delta32/Delta32 stem-cell transplantation. *N Engl J Med* **360**: 692–698.
10. Allers, K, Hutter, G, Hofmann, J, Loddenkemper, C, Rieger, K, Thiel, E *et al.* (2011). Evidence for the cure of HIV infection by CCR5Delta32/Delta32 stem cell transplantation. *Blood* **117**: 2791–2799.
11. Sarver, N and Rossi, J (1993). Gene therapy: a bold direction for HIV-1 treatment. *AIDS Res Hum Retroviruses* **9**: 483–487.
12. Dropulić, B and Jeang, KT (1994). Gene therapy for human immunodeficiency virus infection: genetic antiviral strategies and targets for intervention. *Hum Gene Ther* **5**: 927–939.
13. Levine, BL, Humeau, LM, Boyer, J, MacGregor, RR, Rebello, T, Lu, X *et al.* (2006). Gene transfer in humans using a conditionally replicating lentiviral vector. *Proc Natl Acad Sci USA* **103**: 17372–17377.
14. Morris, KV and Rossi, JJ (2006). Lentivirus-mediated RNA interference therapy for human immunodeficiency virus type 1 infection. *Hum Gene Ther* **17**: 479–486.
15. Rossi, JJ, June, CH and Kohn, DB (2007). Genetic therapies against HIV. *Nat Biotechnol* **25**: 1444–1454.
16. van Lunzen, J, Glaunsinger, T, Stahmer, I, von Baehr, V, Baum, C, Schilz, A *et al.* (2007). Transfer of autologous gene-modified T cells in HIV-infected patients with advanced immunodeficiency and drug-resistant virus. *Mol Ther* **15**: 1024–1033.
17. Li, MJ, Kim, J, Li, S, Zaia, J, Yee, JK, Anderson, J *et al.* (2005). Long-term inhibition of HIV-1 infection in primary hematopoietic cells by lentiviral vector delivery of a triple combination of anti-HIV shRNA, anti-CCR5 ribozyme, and a nucleolar-localizing TAR decoy. *Mol Ther* **12**: 900–909.
18. Hoxie, JA and June, CH (2012). Novel cell and gene therapies for HIV. *Cold Spring Harb Perspect Med* **2**: a007179.
19. Cannon, P and June, C (2011). Chemokine receptor 5 knockout strategies. *Curr Opin HIV AIDS* **6**: 74–79.
20. Tebas, P, Stein, D, Binder-Scholl, G, Mukherjee, R, Brady, T, Rebello, T *et al.* (2013). Antiviral effects of autologous CD4 T cells genetically modified with a conditionally replicating lentiviral vector expressing long antisense to HIV. *Blood* **121**: 1524–1533.
21. Chono, H, Matsumoto, K, Tsuda, H, Saito, N, Lee, K, Kim, S *et al.* (2011). Acquisition of HIV-1 resistance in T lymphocytes using an ACA-specific E. coli mRNA interferase. *Hum Gene Ther* **22**: 35–43.
22. Shimazu, T, Degenhardt, K, Nur-E-Kamal, A, Zhang, J, Yoshida, T, Zhang, Y *et al.* (2007). NBK/BIK antagonizes MCL-1 and BCL-XL and activates BAK-mediated apoptosis in response to protein synthesis inhibition. *Genes Dev* **21**: 929–941.
23. Okamoto, M, Chono, H, Kawano, Y, Saito, N, Tsuda, H, Inoue, K *et al.* (2013). Sustained inhibition of HIV-1 replication by conditional expression of the *E. coli*-derived endoribonuclease MazF in CD4+ T cells. *Hum Gene Ther Methods* **24**: 94–103.

24. Berkhout, B, Silverman, RH and Jeang, KT (1989). Tat trans-activates the human immunodeficiency virus through a nascent RNA target. *Cell* **59**: 273–282.
25. Chono, H, Saito, N, Tsuda, H, Shibata, H, Ageyama, N, Terao, K *et al.* (2011). *In vivo* safety and persistence of endoribonuclease gene-transduced CD4+ T cells in cynomolgus macaques for HIV-1 gene therapy model. *PLoS One* **6**: e23585.
26. Reimann, KA, Li, JT, Voss, G, Lekutis, C, Tenner-Racz, K, Racz, P *et al.* (1996). An env gene derived from a primary human immunodeficiency virus type 1 isolate confers high *in vivo* replicative capacity to a chimeric simian/human immunodeficiency virus in rhesus monkeys. *J Virol* **70**: 3198–3206.
27. Pitcher, CJ, Hagen, SI, Walker, JM, Lum, R, Mitchell, BL, Maino, VC *et al.* (2002). Development and homeostasis of T cell memory in rhesus macaque. *J Immunol* **168**: 29–43.
28. Klebanoff, CA, Gattinoni, L, Torabi-Parizi, P, Kerstann, K, Cardones, AR, Finkelstein, SE *et al.* (2005). Central memory self/tumor-reactive CD8+ T cells confer superior antitumor immunity compared with effector memory T cells. *Proc Natl Acad Sci USA* **102**: 9571–9576.
29. Zhang, Y, Zhang, J, Hoeflich, KP, Ikura, M, Qing, G and Inouye, M (2003). MazF cleaves cellular mRNAs specifically at ACA to block protein synthesis in *Escherichia coli*. *Mol Cell* **12**: 913–923.
30. Ranga, U, Woffendin, C, Verma, S, Xu, L, June, CH, Bishop, DK *et al.* (1998). Enhanced T cell engraftment after retroviral delivery of an antiviral gene in HIV-infected individuals. *Proc Natl Acad Sci USA* **95**: 1201–1206.
31. Schmidt, M, Zickler, P, Hoffmann, G, Haas, S, Wissler, M, Muessig, A *et al.* (2002). Polyclonal long-term repopulating stem cell clones in a primate model. *Blood* **100**: 2737–2743.
32. Ahr, B, Robert-Hebmann, V, Devaux, C and Biard-Piechaczyk, M (2004). Apoptosis of uninfected cells induced by HIV envelope glycoproteins. *Retrovirology* **1**: 12.
33. Primate Society of Japan (1986). Guiding principles for animal experiments using nonhuman primates. *Primate Res* **2**: 111–113.
34. Honjo, S (1985). The Japanese Tsukuba Primate Center for Medical Science (TPC): an outline. *J Med Primatol* **14**: 75–89.
35. Akiyama, H, Ido, E, Akahata, W, Kuwata, T, Miura, T and Hayami, M (2003). Construction and *in vivo* infection of a new simian/human immunodeficiency virus chimera containing the reverse transcriptase gene and the 3' half of the genomic region of human immunodeficiency virus type 1. *J Gen Virol* **84**(Pt 7): 1663–1669.
36. Lee, JT, Yu, SS, Han, E, Kim, S and Kim, S (2004). Engineering the splice acceptor for improved gene expression and viral titer in an MLV-based retroviral vector. *Gene Ther* **11**: 94–99.
37. Verzeletti, S, Bonini, C, Marktel, S, Nobili, N, Ciceri, F, Traversari, C *et al.* (1998). Herpes simplex virus thymidine kinase gene transfer for controlled graft-versus-host disease and graft-versus-leukemia: clinical follow-up and improved new vectors. *Hum Gene Ther* **9**: 2243–2251.
38. Ageyama, N, Kimikawa, M, Eguchi, K, Ono, F, Shibata, H, Yoshikawa, Y *et al.* (2003). Modification of the leukapheresis procedure for use in rhesus monkeys (Macaca mulata). *J Clin Apher* **18**: 26–31.

Supplementary Information accompanies this paper on the Molecular Therapy–Nucleic Acids website (http://www.nature.com/mtna)

ORIGINAL RESEARCH

American Heart Association | American Stroke Association.

Tenascin-C Aggravates Autoimmune Myocarditis via Dendritic Cell Activation and Th17 Cell Differentiation

Tomoko Machino-Ohtsuka, MD; Kazuko Tajiri, MD, PhD; Taizo Kimura, MD, PhD; Satoshi Sakai, MD, PhD; Akira Sato, MD; Toshimichi Yoshida, MD, PhD; Michiaki Hiroe, MD, PhD; Yasuhiro Yasutomi, DVM, PhD; Kazutaka Aonuma, MD, PhD; Kyoko Imanaka-Yoshida, MD, PhD

Background—Tenascin-C (TN-C), an extracellular matrix glycoprotein, appears at several important steps of cardiac development in the embryo, but is sparse in the normal adult heart. TN-C re-expresses under pathological conditions including myocarditis, and is closely associated with tissue injury and inflammation in both experimental and clinical settings. However, the pathophysiological role of TN-C in the development of myocarditis is not clear. We examined how TN-C affects the initiation of experimental autoimmune myocarditis, immunologically.

Methods and Results—A model of experimental autoimmune myocarditis was established in BALB/c mice by immunization with murine α-myosin heavy chains. We found that TN-C knockout mice were protected from severe myocarditis compared to wild-type mice. TN-C induced synthesis of proinflammatory cytokines, including interleukin (IL)-6, in dendritic cells via activation of a Toll-like receptor 4, which led to T-helper (Th)17 cell differentiation and exacerbated the myocardial inflammation. In the transfer experiment, dendritic cells loaded with cardiac myosin peptide acquired the functional capacity to induce myocarditis when stimulated with TN-C; however, TN-C-stimulated dendritic cells generated from Toll-like receptor 4 knockout mice did not induce myocarditis in recipients.

Conclusions—Our results demonstrated that TN-C aggravates autoimmune myocarditis by driving the dendritic cell activation and Th17 differentiation via Toll-like receptor 4. The blockade of Toll-like receptor 4-mediated signaling to inhibit the proinflammatory effects of TN-C could be a promising therapeutic strategy against autoimmune myocarditis. **(*J Am Heart Assoc.* 2014;3:e001052 doi: 10.1161/JAHA.114.001052)**

Key Words: dendritic cell • myocarditis • tenascin-C • Th17 • TLR4

Myocarditis is induced by a variety of agents, including toxins, alcohols, parasites, bacteria, and viruses.[1,2] Postinfectious autoimmune myocarditis often results in idiopathic dilated cardiomyopathy (DCM), which is sometimes a lethal disorder characterized by left ventricular (LV) enlargement and systolic dysfunction.[1,2]

From the Cardiovascular Division, Faculty of Medicine, University of Tsukuba, Japan (T.M.-O., K.T., T.K., S.S., A.S., K.A.); Mie University Research Center for Matrix Biology and Department of Pathology and Matrix Biology, Mie University Graduate School of Medicine, Tsu, Japan (T.Y., K.I.-Y.); Department of Cardiology, National Center of Global Health and Medicine, Tokyo, Japan (M.H.); Laboratory of Immunoregulation and Vaccine Research, Tsukuba Primate Research Center, National Institution of Biomedical Innovation, Tsukuba, Japan (Y.Y.).

Correspondence to: Kazutaka Aonuma, MD, PhD, Cardiovascular Division, Faculty of Medicine, University of Tsukuba, 1-1-1 Tennodai, Tsukuba 305-8575, Japan. E-mail: kaonuma@md.tsukuba.ac.jp

Received July 14, 2014; accepted August 7, 2014.

Experimental autoimmune myocarditis (EAM) is a mouse model of such a kind of inflammation-based cardiomyopathy.[3,4] EAM is known as a $CD4^+$ T-cell-mediated disease, and activation of self-antigen-loaded dendritic cells (DCs) is critical for the expansion of autoreactive $CD4^+$ T cells.[5] Upon encountering immunologic danger, the maturated and activated DCs act as an important commander regulating naïve $CD4^+$ T cells by means of antigen presentation, costimulatory molecule engagement, and release of a cocktail of polarizing cytokines.[6] DC activation is mediated by the recognition of pathogen-associated molecular patterns and damage-associated molecular patterns, which are sensed by pattern-recognized receptors such as Toll-like receptors (TLRs).[6]

Recently, accumulating evidence has highlighted the proinflammatory role of several extracellular matrix molecules including tenascin-C (TN-C), osteopontin, and galectin.[7–10] Of these, TN-C acts as a damage-associated molecular pattern and directly activates inflammatory cells including lymphocytes, macrophages, synovial fibroblasts, and DCs.[11–14] TN-C is synthesized by various cell types in response to inflammatory cytokines and mechanical

stress.[12,15,16] TN-C is not normally expressed in the adult heart but is specifically upregulated during clinical conditions accompanying inflammation,[7,17] such as acute myocardial infarction,[18] hypertensive cardiac fibrosis,[19] myocarditis,[15,20] and some cases of DCM.[21] In particular, our previous analysis of the myocardium obtained from left ventriculoplasty specimens of patients with DCM showed that about half of the patients had significant active inflammation associated with TN-C expression.[21] Thus, it has been recognized that TN-C is closely associated with inflammatory status in cardiovascular diseases. However, how TN-C acts as a proinflammatory stimulus by mediating the immune system in myocarditis has not been fully understood.

Here, we show that TN-C leads to TLR4-mediated inflammatory responses in DCs and exacerbates myocardial inflammation. TN-C knockout (TNKO) mice were protected from severe myocarditis in a model of cardiac myosin-induced autoimmune myocarditis. Furthermore, we found that TN-C induced synthesis of proinflammatory cytokines, including interleukin-6 (IL-6), in DCs via activation of TLR4, which led to Th17 cell differentiation. Finally, in the transfer experiment, DCs loaded with cardiac myosin peptide acquired the functional capacity to induce myocarditis when stimulated with TN-C; however, TN-C-stimulated DCs generated from TLR4 knockout (TLR4KO) mice did not induce myocarditis in recipients.

Materials and Methods

Mice

TNKO mice, originally generated by Saga et al., were backcrossed with BALB/c mice for more than 12 generations.[22] Male TNKO mice and wild-type (WT) littermates (5 to 7 weeks of age) were used in the experiments. Other male BALB/c mice (same age) that were used to obtain bone marrow cells were purchased from CLEA Japan. TLR4KO mice were purchased from Oriental Yeast. All animal experiments were approved by the Institutional Animal Experiment Committee of the University of Tsukuba.

Induction of EAM

The mice were immunized with 100 μg of α-myosin H-chain peptide (MyHC-α) (MyHC-$\alpha_{614-629}$ [Ac-RSLKLMATLFSTYA-SADR-OH]; Toray Research Center) emulsified 1:1 in a PBS/complete Freund's adjuvant (1 mg/mL; H37Ra; Sigma-Aldrich) on days 0 and 7, as described previously.[23] At different time points (0, 2, 5, 8, 11, 14, 17, 21, 25, 29, and 33 days) after the first immunization, a total of 44 mice were anesthetized with pentobarbital (60 mg/kg i.p.) and their hearts were removed.

Myosin-Specific Bone Marrow-Derived Dendritic Cell (BMDC)-Induced Myocarditis

BMDCs were generated as previously described.[24] BMDCs were pulsed overnight with 10 μg/mL MyHC-α peptide and stimulated for another 4 hours with 1 μg/mL lipopolysaccharide (LPS) (Sigma-Aldrich) or 10 μg/mL TN-C and 5 μg/mL anti-CD40L (AbD Serotec).[5] Recipient mice received 5×10^5 pulsed and activated BMDCs i.p. on days 0, 2, and 4 and were killed 10 days after the first injection.

Histopathological and Immunohistochemical Examination

The hearts were fixed in 4% paraformaldehyde in PBS and embedded in paraffin wax. For a histological analysis, 3-μm-thick sections were cut and stained with hematoxylin and eosin. To evaluate the expression of TN-C, we performed immunohistochemistry as previously described.[25] In brief, sections after antigen retrieval were incubated with polyclonal rabbit anti-TN-C antibodies,[15,26] followed by treatment with horseradish peroxidase–conjugated goat anti-rabbit antibody (MBL, Nagoya, Japan). The antibody reactions were visualized using diaminobenzidine chromogen and were counterstained with hematoxylin. Myocarditis severity was scored on hematoxylin and eosin–stained sections using grades from 0 to 4: 0, no inflammation; 1, >25% of the heart section involved; 2, 25% to 50%; 3, >50% to 75%; and 4, >75%, as described previously.[23] Two independent researchers scored the slides separately in a blinded manner.

Assessment of LV Function

The assessment of the LV function was performed in naïve or EAM WT and TNKO mice (14 days after immunization). The mice were anesthetized with an intraperitoneal injection of sodium pentobarbital (50 mg/kg). The LV apex was exposed via a subdiaphragmatic incision. An apical stab was made with a 27-gauge needle containing a fiber pressure sensor (FPI-LS-PT9; FISO Technologies, Inc, Québec, Canada),[27] placed to span the long axis of the LV. Pressure measurements were obtained at steady state. All signals were analyzed with a signal conditioner (FPI-LS-10; FISO Technologies, Inc) and data acquisition system (LabTrax 4, World Precision Instruments, Sarasota, FL) and then stored on disks for off-line analysis using software (LabScribe, iWorx Systems, Inc, Dover, NH). The following indices were assessed: heart rate, systolic and end-diastolic LV pressures, and maximal and minimum rates of LV pressure development (±dP/dt).

Flow Cytometric Analyses and Intracellular Cytokine Staining

Heart inflammatory cells were isolated and processed as previously described.[5,28] For the flow cytometric analysis of the surface markers and cytoplasmic cytokines, the cells were stained directly using fluorochrome-conjugated mouse-specific antibodies and analyzed with a FACSCalibur instrument (BD Biosciences). For the analysis of the intracellular cytokine production, the cells were stimulated with 50 ng/mL phorbol 12-myristate 13-acetate (Sigma-Aldrich), 750 ng/mL ionomycin (Sigma-Aldrich), and 10 μg/mL brefeldin A (eBioscience) for 5 hours. The antibodies were purchased from eBioscience and included CD4, CD45, Forkhead box protein (Foxp)3, interferon (IFN)-γ, and IL-17A.

Stimulation of DCs

BMDCs (5×10^5) generated as described above were cultured with TN-C (10 μg/mL) for 48 hours. In some experiments, 0.1 μmol/L TAK242 (Millipore), a selective TLR4 signal transduction inhibitor, was added. Culture supernatants were subjected to measurements of cytokine or chemokine production. For the Western blotting analysis, we used DCs obtained from spleens of naïve WT and TNKO mice by anti-CD11c microbeads (Miltenyi Biotec). To evaluate the TLR4 expression or NF-κB signaling, the DCs were stimulated with TN-C (10 μg/mL) or tumor necrosis factor-α (20 ng/mL) for 15 minutes and were subjected to analysis.

In Vitro Th17 Induction

We used a $CD4^+CD62L^+$ T-cell isolation kit (Miltenyi Biotec) and anti-CD11c microbeads (Miltenyi Biotec) to isolate $CD4^+$ naïve T cells and DCs from spleens, respectively. The $CD4^+$ naïve T cells (1×10^6) were co-cultured with DCs (5×10^4) and stimulated with 10 μg/mL TN-C for 72 hours. In some experiments, DCs were pretreated with TAK242 (0.1 μmol/L) or anti-IL-6 antibody (10 μg/mL; R&D Systems). The supernatants were collected and the cytokines were measured.

Measurements of Cytokines and Chemokines

The hearts were homogenized in media containing 10% fetal bovine serum. The supernatants were collected after centrifugation and stored at −80°C. The concentrations of cytokines and chemokines in the heart homogenates, serum, or culture supernatants were measured by the use of Millipore multiplex immunoassay panels (Millipore). In some cases, the cytokine levels were confirmed with a Quantikine ELISA kit (R&D Systems). For measurements of the TN-C concentration, the hearts were homogenized in a buffer containing 150 mmol/L NaCl, 25 mmol/L Tris (pH 7.4), 5 mmol/L EDTA, 10 mmol/L sodium pyrophosphate, 10 mmol/L NaF, 1 mmol/L Na_3NO_4, and complete miniprotease inhibitors (Roche). The proteins were extracted from the homogenized samples by adding Triton X-100 (Sigma) to a final concentration of 1%. Suspensions of hearts mixed with 1% Triton X were vortexed and incubated on ice for 2 hours. Then, the suspensions were centrifuged at 22 200 g for 15 minutes, and the supernatants were collected. The concentration of the TN-C was measured by a Tenascin-C Large (FNIII-B) Assay kit (IBL).

Serum Troponin Determinations

Blood was collected from mice at the time of sacrifice, and the serum levels of cardiac troponin I were measured with an ELISA kit (Mouse Cardiac Tn-I, Ultra Sensitive; Life Diagnostics).

Western Blot Analysis

The total lysates from WT and TNKO DCs were immunoblotted and probed with primary antibodies against TLR4, NF-κB, and phospho-NF-κB (Ser536) (Cell Signaling Technology). Horseradish peroxidase–conjugated secondary antibodies (Cell Signaling Technology) were used to identify the binding sites of the primary antibody.

RNA Extraction and Quantitative Real-Time Reverse Transcription Polymerase Chain Reaction

All of the hearts removed for the reverse transcription polymerase chain reaction were snap frozen and stored at −80°C. For the preparation of the total RNA, the tissue was homogenized using a bead kit (MagNA Lyser Green Beads; Roche Diagnostics) according to the manufacturer's instructions. The total RNA was extracted using a MagNA Pure Compact Instrument (Roche Applied Science) together with a MagNA Pure Compact RNA Isolation Kit (Roche Applied Science) according to the manufacturer's instructions. cDNA was synthesized from 1 μg total RNA with an Omniscript RT kit (Qiagen). A quantitative-reverse transcription polymerase chain reaction analysis was performed with the LightCycler 480 system (Roche Applied Science) with a Universal Probe Library (Roche Applied Science). The primers for the mouse *Tnc* were 5′-CCCTCTCTCTGTTGAGGTCTTG-3′ (sense) and 5′-CCCAGCTGACCTCAGTCAC-3′ (antisense). The primers for the mouse *Hprt* were 5′-TCCTCCTCAGACCGCTTTT-3′ (sense) and 5′-CCTGGTTCATCATCGCTAATC-3′ (antisense). *Hprt* RNA was used as an internal control.

Statistics

All data are expressed as means±SEM. The normality was tested with the Shapiro–Wilk test. The TN-C mRNA and protein levels after the myocarditis induction were compared with the baseline levels using an unpaired 2-tailed t test (Figure 1B). The heart-to-body-weight ratios, serum troponin I concentrations, flow cytometric analyses data, hemodynamic parameters, and cytokines/chemokine levels were compared between 2 groups by an unpaired 2-tailed *t* test (Figures 2C through 2H, 3, 4, 5B through 5D, 6, and 8C and 8D). A 1-way analysis of variance was used to compare the levels of the TN-C in multiple groups (Figure 5A). To compare the severity scores of myocarditis between 2 groups, the Mann–Whitney *U* test was used (Figures 2B, 8B, and Table). The Fisher Exact test was used to compare the prevalence of DC-induced myocarditis between the control group and the other 4 groups, respectively (Table). A value of $P<0.05$ was considered to be statistically significant.

Results

Expression of TN-C in the EAM Hearts

First, we examined the expression of TN-C in WT mice with EAM that was induced by immunization with cardiac myosin. Around 5 to 6 days after the first immunization, small clusters of infiltrating inflammatory cells appeared, and TN-C became detectable (Figure 1A). The TN-C expression peaked at day 14, and the molecule was localized to the interstitial spaces in areas where inflammatory cell infiltration was evident (Figure 1A). The myocardial inflammation and TN-C expression gradually subsided and disappeared around 25 days after immunization (Figure 1A). A quantitative-reverse transcription polymerase

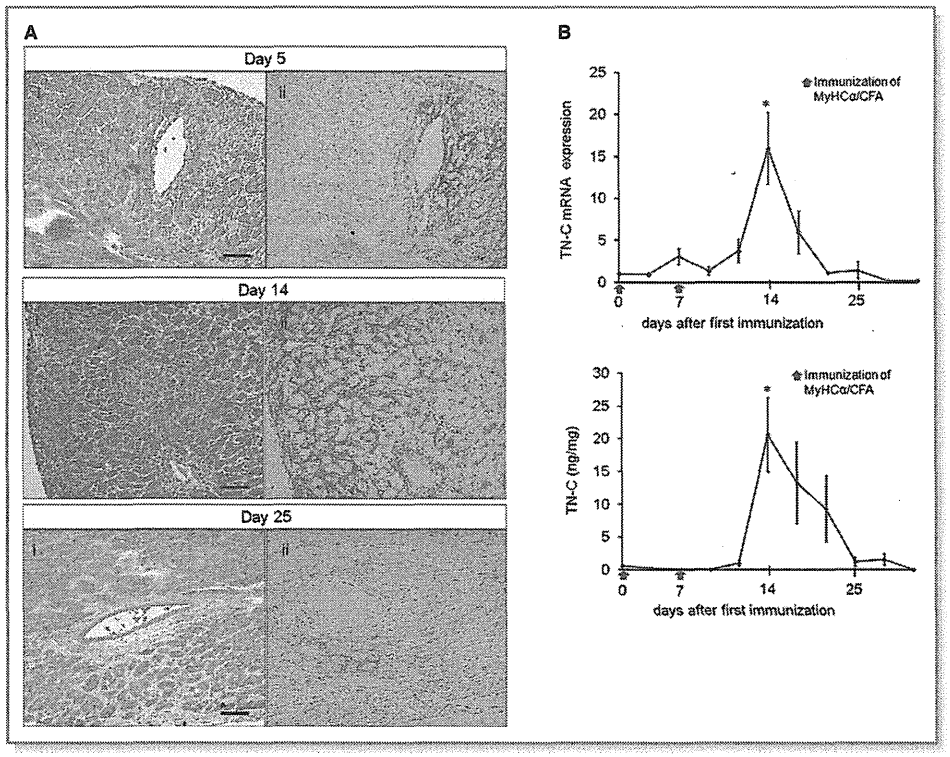

Figure 1. Tenascin-C (TN-C) expression in cardiac myosin-induced autoimmune myocarditis. BALB/c mice were immunized twice, on days 0 and 7, with 100 μg of cardiac myosin epitope peptide (MyHC-α). A, Representative histology of myocarditis on days 5, 14, and 25, respectively. Hematoxylin and eosin staining (i) and immunostaining for TN-C (ii). Scale bars=50 μm. B, The expression of TN-C in hearts obtained from immunized mice at the indicated time points. Immunization on days 0 and 7 are indicated with red arrows. TN-C mRNA expression was evaluated by quantitative reverse transcription–polymerase chain reaction. The results are reported as the fold change in the gene expression relative to the expression on day 0. The TN-C protein levels were measured by an ELISA. n=4 per group at each time point. Error bars represent the mean±SEM. **P*<0.05 vs day 0. CFA indicates complete Freund's adjuvant.

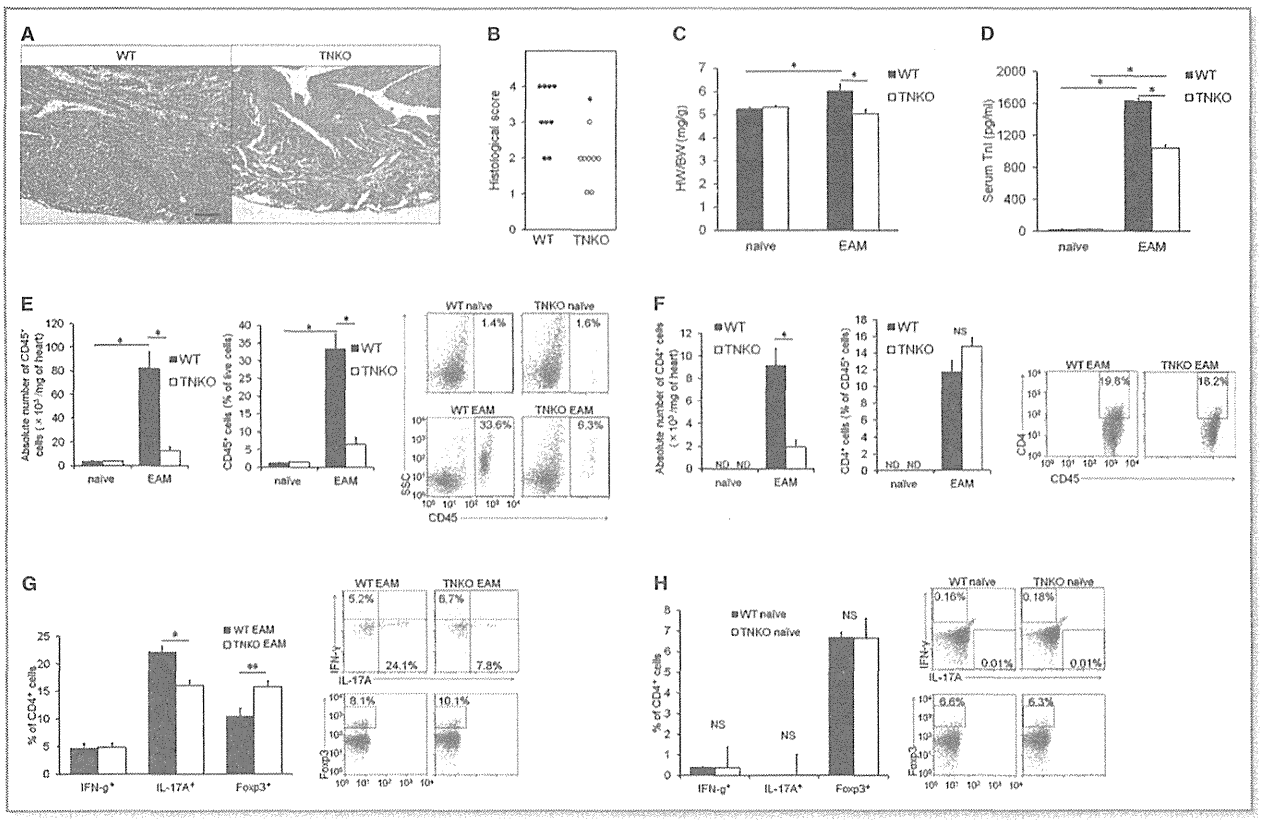

Figure 2. Tenascin-C (TN-C) deficiency inhibits inflammation in the heart. Wild-type (WT) and TN-C knockout (TNKO) mice were immunized with cardiac myosin peptide on days 0 and 7. A, Representative hematoxylin and eosin–stained sections of hearts on day 14 from WT and TNKO mice. Scale bar=100 μm. B, Severity of myocarditis in the heart sections. C, Heart-to-body-weight ratios (HW/BW) in WT and TNKO mice before and after experimental autoimmune myocarditis (EAM) induction (day 14). D, Circulating troponin I (TnI) concentration of WT and TNKO mice before and after EAM induction (day 14). E through G, Inflammatory cells infiltrating the heart were isolated and analyzed by flow cytometry of WT and TNKO mice before and after EAM induction (on day 14). E, Absolute number of $CD45^+$ cells, frequency of $CD45^+$ cells within live cells, and representative plots are shown. F, Absolute number of $CD4^+$ cells, frequency of $CD4^+$ cells within $CD45^+$ cells, and representative plots are shown. Representative plots (gated on $CD4^+$ T cells) and the frequency of both the interferon (IFN)-γ^+ (Th1), interleukin (IL)-17^+ (Th17), and $Foxp3^+$ (regulatory T-cell) cells among all $CD4^+$ cells (G) are shown. n=5 to 8 per group (B through G). H, Splenocytes in naïve WT and TNKO mice were isolated and analyzed by a flow cytometric analysis. Representative plots (gated on $CD4^+$ T cells) and the frequency of the IFN-γ^+ (Th1), IL-17^+ (Th17), and $Foxp3^+$ cells among all $CD4^+$ cells is shown. n=4 per group. The bar graphs show the group mean±SEM. The results of 1 of 2 representative experiments are shown. *P<0.01, **P<0.05. Foxp indicates Forkhead box protein; ND, not detected; SSC, side scatter.

chain reaction analysis and ELISA showed that TN-C was expressed in parallel with the histological findings (Figure 1B).

TNKO Mice Are Protected From Progression of EAM

To determine whether TN-C contributed to the progression of myocarditis, we compared the severity of myocarditis in WT and TNKO mice. On day 14 after immunization, when the TN-C expression had peaked, a histopathological examination revealed larger areas occupied by heart-infiltrating cells in the myocardium of WT mice compared with TNKO mice (Figure 2A). TNKO mice had a significantly lower myocarditis severity score than did the WT mice (Figure 2B). The heart-to-body-weight ratio in the EAM-TNKO mice had significantly decreased compared with that in the EAM-WT mice (Figure 2C), as did the level of circulating cardiac troponin I, a clinical marker of cardiomyocyte damage,[29] but these parameters were comparable between the WT and TNKO mice at baseline (Figure 2D). A flow cytometric analysis of the heart infiltrates revealed an attenuation of the inflammatory cells ($CD45^+$ leukocytes) in TNKO mice compared with that in WT mice (Figure 2E). No difference was found in the percentage of $CD4^+$ T cells among the $CD45^+$ cells between both groups (Figure 2F). Intracellular staining of the $CD4^+$ cells revealed that the proportion of IL-$17A^+$ cells (Th17) was higher and that of $Foxp3^+$ cells (regulatory T cells) was lower in WT than TNKO mice,

Table. Prevalence and Severity of MyHC-α-Loaded DC-Induced Myocarditis in WT and TN-C KO Mice

Donors	Recipients	Activation	Prevalence (Day 10)	Median Severity Grade at Day 10 (Individual Data)
WT	WT	PBS	0/7	0
WT	WT	LPS	7/7*	2 (2, 2, 2, 2, 3, 3, 3)†
WT	WT	TN-C	7/7*	2 (1, 2, 2, 2, 3, 3, 3)†
TNKO	TNKO	PBS	0/7	0
TNKO	TNKO	TN-C	7/7*	2 (1, 1, 2, 2, 2, 3, 3)†

DC indicates dendritic cell; LPS, lipopolysaccharide; MyHC-α, α-myosin H-chain peptide; TN-C, tenascin-C; TNKO, TN-C knockout; WT, wild-type.
*P<0.001 (Fisher's exact test), †P<0.01 (Mann-Whitney U test) vs WT-DCs (with PBS)-induced myocarditis.

whereas the proportion of IFN-γ^+ cells (Th1) was similar between WT and TNKO mice (Figure 2G). The $CD4^+$ T-cell proportions in splenocytes at day 0 did not differ between WT and TNKO mice (Figure 2H), indicating that the deficiency of TN-C did not influence $CD4^+$ T-cell differentiation in the non-EAM condition. To further evaluate the effects of TN-C deficiency on the severity of EAM, we examined hemodynamic parameters using a pressure sensor. In the naïve mice, there was no statistical difference in the heart rate, LV systolic pressure, LV end-diastolic pressure, or ±dP/dt between the WT and TNKO mice (Figure 3A through 3E). The LV end-diastolic pressure increased and ±dP/dt decreased more in the WT EAM mice than in the WT naïve mice, consistent with severe myocarditis (Figure 3B through 3E). In comparison, TNKO mice showed no significant deterioration in these parameters even after the induction of EAM (Figure 3B through 3E).

Taken together, the presence of TN-C in the heart during the acute phase of EAM might contribute to the infiltration of inflammatory cells including Th17 into the heart and to the progression of myocarditis and LV dysfunction.

TN-C Promotes Proinflammatory Cytokine and Chemokine Synthesis in the Heart

To gain new insights into the mechanism of protection against myocarditis in TNKO mice, we examined whether a TN-C deficiency affected the cytokine and chemokine milieu in the heart. In naive WT and TNKO hearts, the expression of proinflammatory cytokines and chemokines was quite small to none (Figure 4). On day 14 following immunization, the heart homogenates from TNKO mice had significantly reduced levels of the proinflammatory cytokines IL-1α, IL-1β, IL-6, IL-17, tumor necrosis factor-α, and transforming growth factor-β

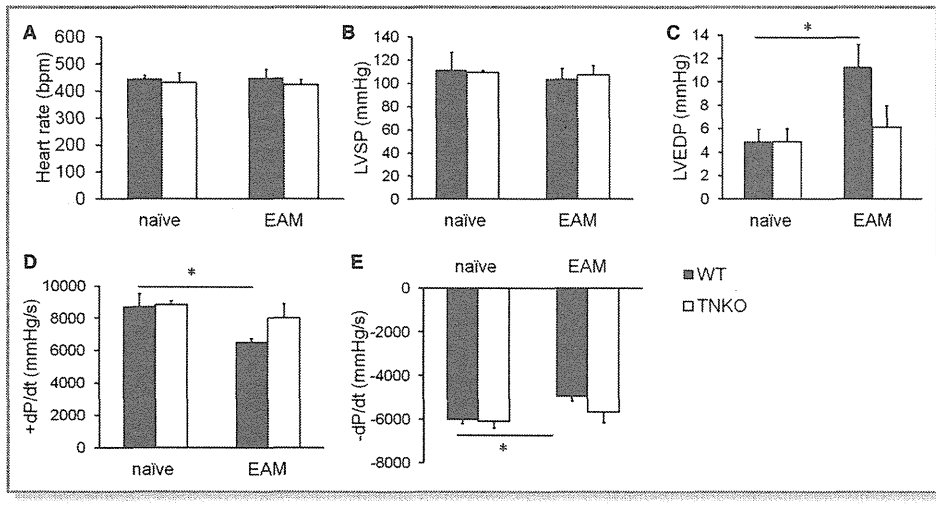

Figure 3. Effects of tenascin-C (TN-C) deficiency on the hemodynamic parameters in experimental autoimmune myocarditis (EAM) mice. A, Heart rate; (B) Left ventricular (LV) systolic pressure (LVSP); (C) LV end-diastolic pressure (LVEDP); (D) Maximal rate of the increase in the LV pressure (+dP/dt); and (E), Maximal rate of the decrease in the LV pressure (−dP/dt). Naïve or EAM wild-type (WT) and TN-C knockout (TNKO) mice (day 14) were analyzed. n=5 to 7 per group. Bar graphs show the group mean±SEM. *P<0.05.

DOI: 10.1161/JAHA.114.001052

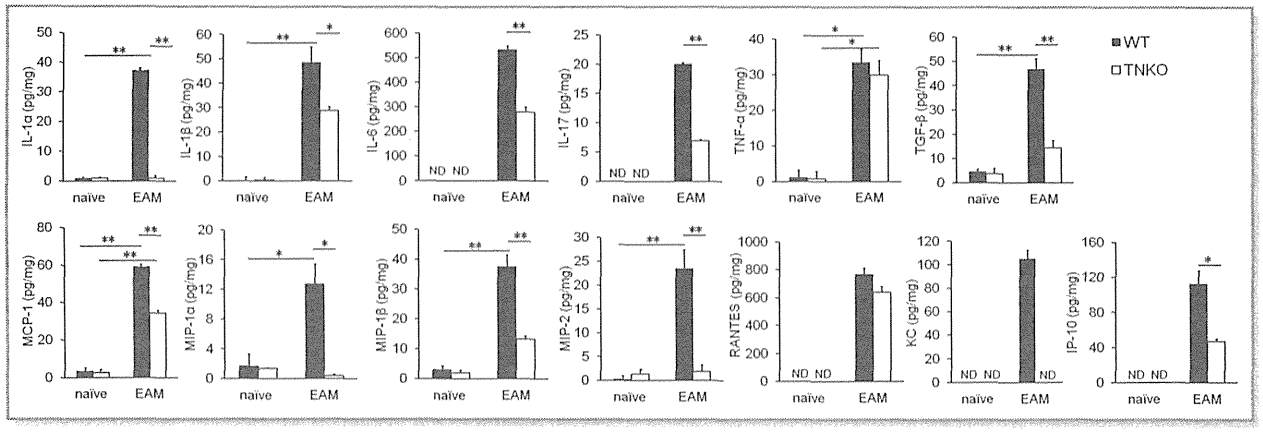

Figure 4. *Tenascin-C (TN-C) deficiency affected the cytokine milieu in the heart. Cytokine and chemokine secretion in homogenized hearts* obtained from naïve and experimental autoimmune myocarditis (EAM) (on day 14) wild-type (WT) and TN-C knockout (TNKO) mice was assessed by an ELISA. n=4 to 5 per group. The bar graphs show the group mean±SEM. The results of 1 of 2 representative experiments are shown. **P*<0.05, ***P*<0.01. IL indicates interleukin; IP, IFN-γ-induced protein; KC, keratinocyte chemoattractant; MCP, monocyte chemoattractant protein; MIP, macrophage inflammatory protein; ND, not detected; RANTES, regulated on activation, normal T-cell expressed and secreted; TGF, transforming growth factor; TNF, tumor necrosis factor.

(Figure 4). Also, the lack of TN-C had significantly reduced the levels of the following chemokines: macrophage inflammatory protein (MIP)-1α (CCL3), MIP-1β (CCL4), MIP-2 (CXCL2), monocyte chemoattractant protein-1 (MCP-1), keratinocyte chemoattractant (KC) (CXCL1), and IFN-γ-induced protein (IP)-10 (CXCL10) (Figure 4). Thus, protection from autoimmune myocarditis in TNKO mice is associated with abrogation of proinflammatory molecules and chemokines in the heart.

TN-C Mediates DC Activation and Th17 Cell Development

EAM is a $CD4^+$ T-cell-mediated disease,[3,4] and DCs are the major antigen-presenting cells (and key players in the priming of appropriate $CD4^+$ T-cell responses. To assess whether TN-C is secreted by DCs, we generated BMDCs in vitro by culturing bone marrow cells obtained from WT mice with granulocyte/macrophage colony-stimulating factor. We found that BMDCs activated with LPS produced only a small amount of TN-C, as did nonstimulated BMDCs (Figure 5A). Therefore, we cultured WT BMDCs in the presence of TN-C and investigated the effects of TN-C on BMDCs in proinflammatory cytokine and chemokine production. When BMDCs were stimulated with TN-C, they produced greater amounts of the proinflammatory cytokines IL-1α, IL-1β, IL-6, IL-12p40, and IFN-γ than did those without TN-C (Figure 5B). TN-C stimulation also promoted BMDCs to produce the chemokines MCP-1, MIP-1α, MIP-1β, MIP-2, IP-10, regulated upon activation, normal T-cell expressed and secreted (RANTES), and KC and growth factors G-CSF and granulocyte/macrophage colony-stimulating factor (Figure 5B). These data indicated that TN-C promotes the production of many types of chemokines and inflammatory cytokines from DCs, which participate in the proliferation, accumulation, and activation of immune cells such as monocytes, macrophages, and lymphocytes. Moreover, TN-C induced the production of IL-6, a key cytokine in Th17 development,[30] by BMDCs in a dose-dependent manner (Figure 5C). On the basis of this significant effect of TN-C on IL-6 secretion by DCs, we next attempted to confirm that TN-C-stimulated BMDCs induce Th17 development. We cocultured TN-C-stimulated DCs and naïve $CD4^+$ T cells in the presence of anti-CD3 monoclonal antibody and transforming growth factor-β and analyzed IL-17 production in the culture supernatant. As expected, we found that TN-C-stimulated DCs promoted IL-17 production from $CD4^+$ T cells (Figure 5D). Moreover, we confirmed the neutralization of IL-6 by using a specific antibody that inhibited the effects of TN-C-stimulated DCs on the promotion of IL-17 production from $CD4^+$ T cells (Figure 5D). These results indicated that TN-C encouraged the generation of Th17 via the secretion of IL-6 from DCs.

TN-C Activates DCs via TLR4

Multiple cell-surface receptors are known to bind to the TN-C molecule.[31] Among them, TLR4 has been shown to be a receptor that transmits important signals to modulate inflammatory response.[13] To determine whether TN-C activates DCs via TLR4, we developed BMDCs from TLR4KO mice (TLR4KO-BMDC) and examined whether TN-C induced the cytokine and chemokine secretion. TLR4KO-BMDCs failed to produce the proinflammatory cytokines IL-1α, IL-1β, IL-6, IL-12p40, and IFN-γ even under stimulation with adequate

DOI: 10.1161/JAHA.114.001052

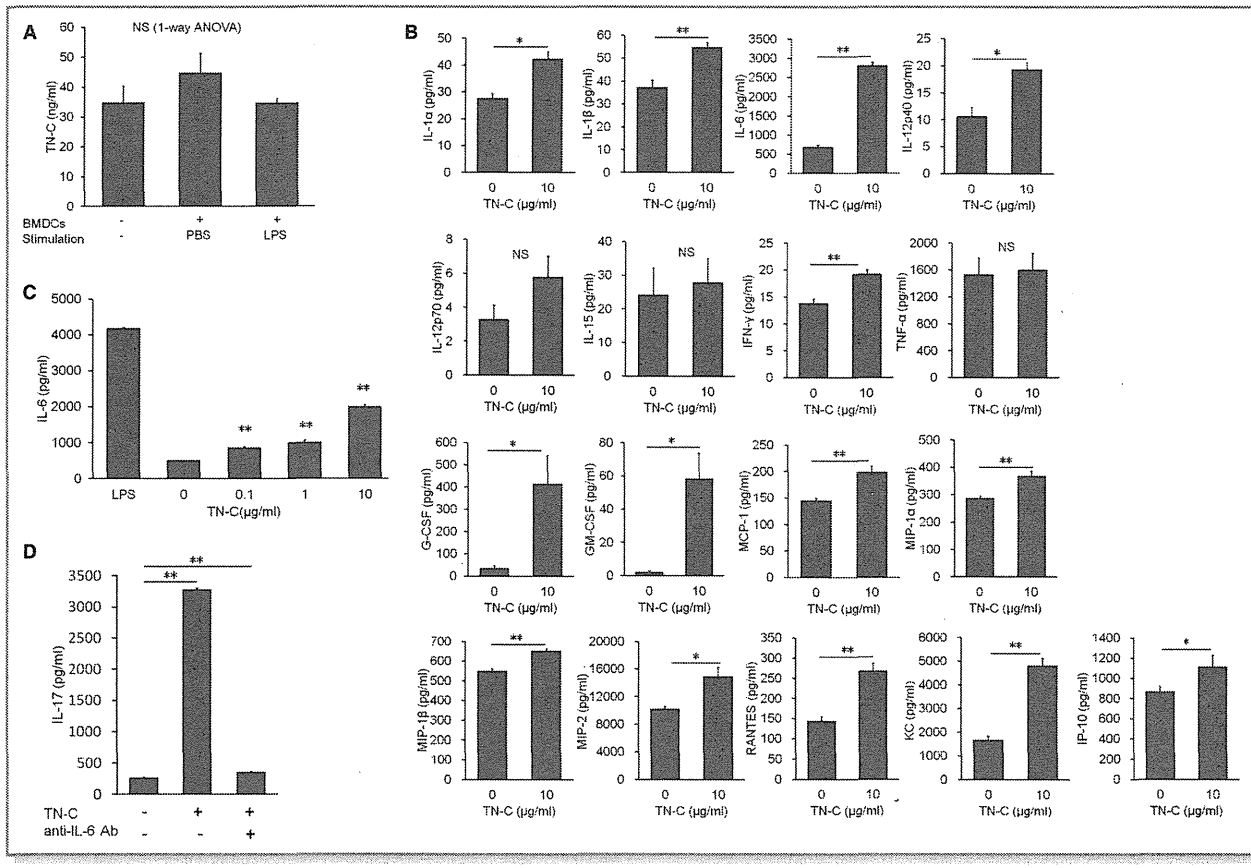

Figure 5. Tenascin-C (TN-C) stimulated production of proinflammatory cytokines and chemokines by bone marrow (BM)–derived dendritic cells (DCs) and differentiated naïve $CD4^+$ cells into Th17 cells. A, DCs generated from BM (BMDCs) were cultured in the presence or absence of lipopolysaccharide (LPS) 1 μg/mL for 72 hours. TN-C secretions from BMDCs and the TN-C concentration in the medium were measured by an ELISA. B, BMDCs were cultured in the presence of 10 μg/mL of TN-C for 48 hours, and the supernatants were subjected to multiplex immunoassay panels for the production of proinflammatory cytokines, chemokines, and growth factors. C, BMDCs were cultured in the presence of the indicated dose of TN-C for 48 hours. TN-C-dose-dependent IL-6 secretions from BMDCs were measured by an ELISA. D, $CD62^{high}$ naïve $CD4^+$ T cells were cultured with DCs, which were obtained from the spleen, in the presence of anti-CD3 mAb (1 μg/mL), TGF-β (2 ng/mL), and TN-C (10 μg/mL) for 72 hours. In some wells, anti-IL-6 Ab (10 μg/mL) was added. The secretion of IL-17 in the supernatants was analyzed by an ELISA. The values are expressed as means±SEM of triplicate culture wells. The results of 1 of 2 representative experiments are shown. $*P<0.05$, $**P<0.01$ (compared to no TN-C stimulation). GM-CSF indicates granulocyte/macrophage colony-stimulating factor; IFN, interferon; IL, interleukin; IP, IFN-γ-induced protein; KC, keratinocyte chemoattractant; MCP, monocyte chemoattractant protein; MIP, macrophage inflammatory protein; NS, not significant; RANTES, regulated on activation, normal T-cell expressed and secreted; TGF, transforming growth factor; TNF, tumor necrosis factor.

amounts of TN-C (Figure 6A). TN-C did not increase the chemokine production, including that of MIP-1α, MIP-1β, MIP-2, RANTES, KC, and IP-10 from TLR4KO-BMDCs (Figure 6A). Furthermore, TLR4 inhibitor TAK242 attenuated TN-C-induced production of IL-1α, IL-1β, IL-6, IL-12p40, IFN-γ, MIP-1α, MIP-1β, MIP-2, RANTES, KC, and IP-10 (Figure 6B). These data indicated that TN-C-activated DCs produce proinflammatory cytokine/chemokine mainly via a TLR4-mediated signaling cascade. Next, we cocultured naïve $CD4^+$ T cells and TN-C-stimulated TLR4KO-BMDCs. Despite the presence of a sufficient amount of TN-C, the IL-17 secretion from $CD4^+$ T cells did not increase (Figure 6C). Furthermore, we cocultured naïve $CD4^+$ T cells and TN-C-stimulated DCs from WT mice with or without TAK242. Pretreatment with TAK242 also resulted in an attenuation of the IL-17 secretion from $CD4^+$ T cells (Figure 6D). Collectively, DCs activated by the TLR4-mediated signaling mainly contributed to the activation of DCs by TN-C, which promoted Th17 differentiation.

TN-C-Stimulated DCs Gain a Myocarditis-Inducing Capacity via TLR4

To collect direct evidence that TN-C provides DCs with the ability to induce autoimmune myocarditis, we used another

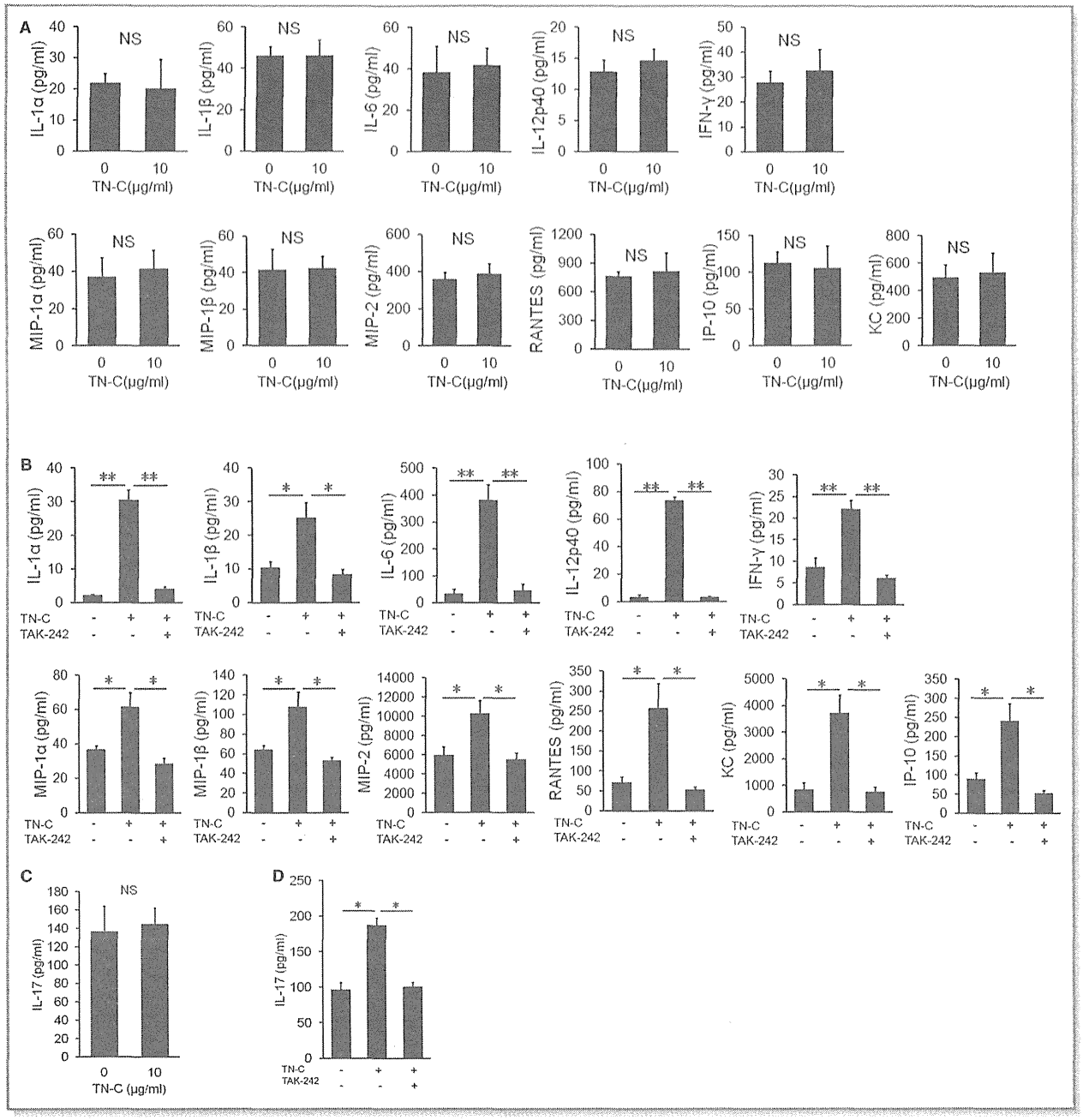

Figure 6. Blocking of toll-like receptor (TLR) 4-mediated tenascin-C (TN-C) signaling reduced the IL-6 secretion and Th17 generation. A, Bone marrow-derived dendritic cells (BMDCs) generated from TLR4 knockout mice were cultured in the presence of 10 μg/mL of TN-C for 48 hours. The supernatants were subjected to an ELISA analysis for the production of proinflammatory cytokines and chemokines. B, BMDCs generated from wild-type mice were cultured in the presence of 10 μg/mL of TN-C for 48 hours. In some wells, TLR4 inhibitor TAK242 (0.1 μmol/L) was added. The supernatants were subjected to an ELISA analysis for the production of proinflammatory cytokines and chemokines. C, $CD62^{high}$ naïve $CD4^+$ T cells were cocultured with BMDCs generated from TLR4 knockout mice in the presence of anti-CD3 mAb (1 μg/mL), TGF-β (2 ng/mL), and full TN-C (10 μg/mL) for 72 hours. The secretion of IL-17 in the supernatants was analyzed by an ELISA. D, $CD62^{high}$ naïve $CD4^+$ T cells were co-cultured with DCs, which were obtained from the spleen, in the presence of anti-CD3 mAb (1 μg/mL), TGF-β (2 ng/mL), and TN-C (10 μg/mL) for 72 hours. In some wells, TLR4 inhibitor TAK242 (0.1 μmol/L) was added. The secretion of IL-17 in the supernatants was analyzed by an ELISA. The values are expressed as means±SEM of triplicate culture wells. The results of 1 of 2 representative experiments are shown. *P<0.05, **P<0.01. IFN indicates interferon; IL, interleukin; IP, IFN-γ-induced protein; KC, keratinocyte chemoattractant; MIP, macrophage inflammatory protein; NS, not significant; RANTES, regulated on activation, normal T-cell expressed and secreted; TGF, transforming growth factor.

DOI: 10.1161/JAHA.114.001052

myocarditis model induced by the transfer of cardiac myosin peptide-loaded BMDCs. In this model, DC-mediated autoimmune myocarditis only occurs when DCs are activated through Toll-like receptors,[5] and it is a useful model to dissect the role of TN-C in the promotion of disease-inducing DCs. Injection of nonstimulated immature DCs did not absolutely generate EAM, whereas injection of TN-C-stimulated WT DCs, and LPS-stimulated DCs induced significant myocarditis at a high prevalence (Table). In addition, nonactivated TNKO-BMDCs could not induce EAM, but exogenous TN-C stimulation of TNKO-BMDCs recovered their ability to induce EAM (Table).

To determine whether TLR4 expression differed between WT and TNKO DCs, we analyzed DCs obtained from the spleen of naïve WT and TNKO mice. In the Western blot analysis, TNKO DCs showed a level of TLR4 expression comparable to that for WT DCs at baseline or in response to TN-C stimulation (Figure 7A). MyD88 and IRAK-1 play crucial roles as adaptor molecules in the signal transduction of TLR4, and the expression of these proteins leads to the activation of NF-κB.[32] To evaluate whether this signaling was altered in the TNKO mice, we examined the difference of NF-κB activation in response to TN-C or tumor necrosis factor-α stimulation between WT and TNKO DCs. TNKO DCs showed no defect in the phosphorylation of NF-κBp65, a major component of NF-κB at serine 536, in response to TN-C or tumor necrosis factor-α stimulation in comparison to WT DCs (Figure 7B). These data confirmed that the protection of TNKO mice from myocarditis did not depend on their insufficient TLR4- or NF-κB-signaling pathways.

As described above, TLR4-mediated signaling mainly contributed to the activation of DCs by TN-C. Therefore, to directly evaluate the role of the TN-C-TLR4 pathway in DCs on disease induction, we stimulated MyHC-α-loaded-BMDCs generated from TLR4KO mice with TN-C and transferred them into recipient mice. As expected, TN-C-stimulated BMDCs from TLR4KO mice failed to induce myocarditis into the recipients (Figure 8A and 8B) with a decreased heart-to-body weight ratio (Figure 8C) and IL-6 production in the heart. (Figure 8D). These results indicated that TN-C activates DCs through TLR4 and exacerbates myocarditis.

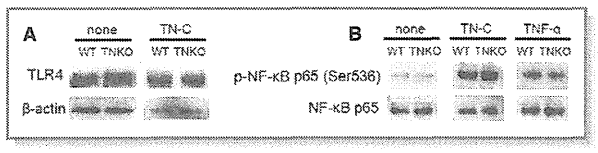

Figure 7. Tenascin-C (TN-C) deficiency does not affect Toll-like receptor (TLR) 4 expression and NF-κB signaling. A, Western blot of TLR4 expression in naïve wild-type (WT) and TN-C knockout (TNKO) DCs left untreated or 15 minutes after stimulation with TN-C (10 μg/mL). B, Western blot of phosphorylation of NF-κB p65 at Ser 536 and NF-κB p65 in naïve WT and TNKO DCs 15 minutes after stimulation with TN-C (10 μg/mL) or TNF-α (20 ng/mL). DCs indicates dendritic cells; TNF, tumor necrosis factor.

Discussion

In the cardiovascular system, TN-C is expressed during embryonic development and plays important roles with regard to the differentiation of cardiomyocytes and angiogenesis.[7,17] TN-C is sparsely detected in normal adults but is upregulated under pathological conditions accompanying tissue injury and inflammation.[7,17] Because of its specific expression style, TN-C has been used to date as a biomarker[33] or a target for nuclear imaging in the diagnosis[20] of myocarditis. With this study, we clearly demonstrated the proinflammatory role of TN-C in the initiation of autoimmune myocarditis. To gain new insights into the immunological influence of TN-C on autoimmune myocarditis, we used models of EAM induced in 2 different ways. The first experiment, using MyHC-α/complete Freund's adjuvant immunization-induced EAM, revealed that the presence of TN-C accelerated myocardial inflammation in vivo. The second experiment, using myosin-specific DC-mediated EAM, provided direct evidence that TN-C is essential for DCs to acquire a sufficient ability to induce autoimmune myocarditis.

DCs are professional antigen-presenting cells and key players in the priming of appropriate antigen-specific T-cell responses against foreign antigens or sometimes self-tissue.[6,34] We directly revealed that TN-C aggravates inflammation through interaction with DCs in EAM, and this finding was similar to that of a previous experiment using an arthritis model.[12] One of the important functions of DCs during inflammation is the production of various pro-inflammatory cytokines.[6] Actually, we found that TN-C-stimulated DCs promoted more production of proinflammatory cytokines than nonstimulated DCs did (Figure 5B), which was similar to previous studies that investigated the effects of TN-C or other extracellular matrix proteins (e.g., osteopontin and galectin-1) on DCs.[12,35–39] Our in vivo study also showed that larger amounts of the pro-inflammatory cytokines IL-1α, IL-1β, and IL-6 were contained in the heart homogenates of EAM WT mice than in EAM TNKO mice (Figure 4). As a result, TNKO mice showed less MyHC-α/complete Freund's adjuvant–induced myocarditis and stable hemodynamic parameters compared to WT mice (Figures 2 and 3). Taken together, TN-C contributed to the progression of EAM through the production of the cytokines IL-1, IL-6, and IL-12p40, which are critically necessary in the pathogenesis of autoimmune heart disease.[40–42] As with the cytokines, TN-C also accelerated the production of chemokines including MCP-1, MIP-1α, MIP-1β,

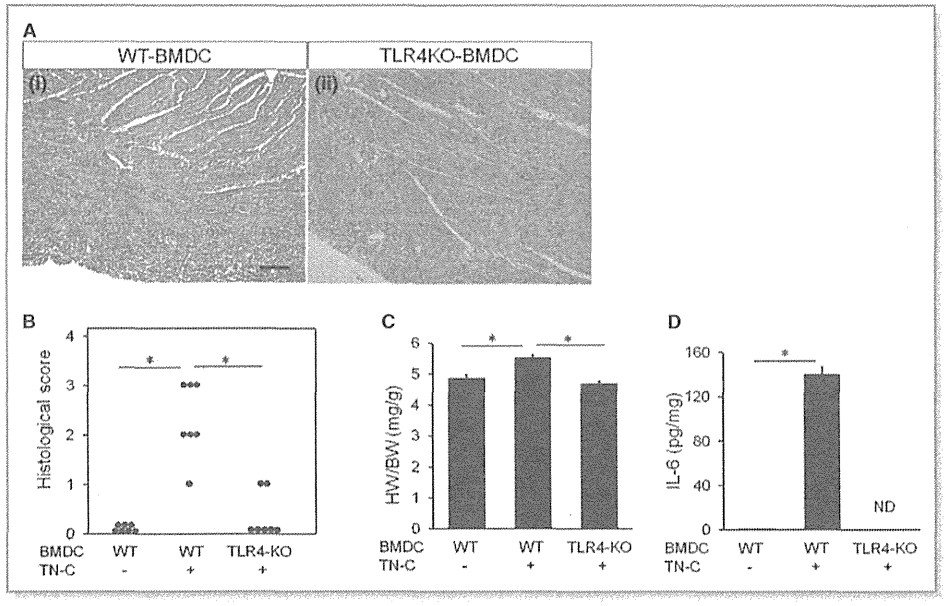

Figure 8. Transfer of myosin-specific bone marrow–derived dendritic cells (BMDCs) generated from Toll-like receptor 4 knockout (TLR4-KO) mice reduced the myocardial inflammation. BMDCs generated from wild-type (WT) or TLR4KO mice were pulsed overnight with 10 μg/mL MyHC-α peptide and stimulated for another 4 hours with 10 μg/mL TN-C and 5 μg/mL anti-CD40L. Recipient mice received 5×10^5 pulsed and activated WT-BMDCs or TLR4KO-BMDCs i.p. on days 0, 2, and 4 and were killed 10 days after the first injection. A, Representative histology (hematoxylin and eosin staining) of the myocarditis on day 10 after the DC transfer. Left image, WT-BMDCs transferred myocarditis, right image, TLR4KO-BMDCs transferred myocarditis. Scale bars=100 μm. B, Severity of myocarditis on day 10 after DC transfer. C, Heart-to-body-weight ratios (HW/BW) on day 10 after DC transfer. D, IL-6 secretion in the homogenized hearts 10 days after BMDC transfer was assessed by an ELISA. The bar graphs show the group mean±SEM. n=7 per group. *P<0.01. IL indicates interleukin; MyHC, myosin H-chain peptide; ND, not detected; TN-C, tenascin-C.

MIP-2, RANTES, KC, and IP-10 by DCs (Figure 5B), and they were also increased more in the hearts of WT EAM mice compared to TNKO EAM mice (Figure 4). In previous experimental myocarditis studies, each of MCP-1,[43] MIP-1α,[43] MIP-1β,[44] MIP-2,[45] RANTES,[44] KC,[46] and IP-10[47] has been identified as a chemotactic factor effecting the infiltration of various inflammatory cells into inflamed tissue. At the site of injury and inflammation, TN-C can provide a scaffold for immune cell adhesion and migration.[10] In fact, our flow cytometric analysis of infiltrating cells into inflamed WT hearts revealed that peak TN-C expression was associated with an increase in infiltrating leukocytes at around 14 days after the first immunization (Figures 1 and 2E through 2G).

We also revealed that TN-C was important for myosin-loaded DCs to acquire the ability to induce EAM. This DC-mediated myocarditis has been established as a model of EAM progression into DCM and heart failure even after resolution of acute inflammatory infiltrates.[5] Consistent with a previous report, our results showed that LPS-stimulated DCs generated significant myocarditis, whereas nonactivated DCs did not (Table).[5] We also showed that stimulation of DCs with TN-C instead of LPS successfully induced EAM at a high prevalence similar to that with LPS stimulation (Table). DC-mediated autoimmunity and heart disease occur only when DCs are activated through Toll-like receptors.[5] Thus, these results suggest that TN-C has an ability comparable to that of LPS for providing DCs with the capacity to induce myocarditis via TLR4 activation. Furthermore, immature BMDCs from TNKO mice did not initiate myocarditis in recipient TNKO mice, but the presence of exogenous TN-C provided TNKO-BMDCs with the full ability to induce EAM (Table). This indicated that the presence of exogenous TN-C is important for acquiring DC activation to induce myocarditis. In clinical settings, myocardial tissues obtained from DCM patients sometimes show active myocarditis without evidence of an active viral invasion into their hearts.[48] Taken together, it is possible that continuous activation of DCs is inducible by extracellular environments regulated in the presence of inflammation even after the active infection and microbe elements in the inflamed heart are diminished.

We showed that activated BMDCs synthesized TN-C at a very low level (Figure 5A), although other published data demonstrated that DCs obtained from peripheral blood or immunized draining lymph nodes can produce TN-C.[12,49]

The differences in the maturation and activation between artificially generated BMDCs and in vivo–derived DCs might have affected the production of TN-C. In the inflamed heart, interstitial fibroblasts at the site of injury are the major source of TN-C.[26,50] TN-C molecules secreted by interstitial cells in the extracellular spaces could modulate immune cell activity in a paracrine fashion.

TN-C influenced the generation of Th17 cells infiltrating into inflamed heart (Figure 2G). Moreover, naïve $CD4^+$ T cells cocultured with TN-C-activated DCs were more differentiated into Th17 cells than were those without TN-C stimulation (Figure 5D). Recently, a subset of IL-17-producing Th17 cells has been described and shown to have a crucial role in the induction of autoimmune tissue injury.[1] Actually, EAM is worsened by the transplantation of Th17 cells, and treatment by IL-17-blocking antibody or active vaccination against IL-17 attenuates the severity of EAM.[28,51] We also found that the frequency of $Foxp3^+$ regulatory T cells was reduced more in the myocardium of WT mice than TNKO mice (Figure 2G). $Foxp3^+$ regulatory T cells inhibit autoimmunity and protect against tissue injury.[52] The current consensus is that IL-6 induces Th17 differentiation together with transforming growth factor-β[30] and is essential for the initiation of EAM through Th17 differentiation.[53,54] Conversely, transforming growth factor-β-mediated conversion of naïve $CD4^+$ cells into $Foxp3^+$ regulatory T cells is strongly inhibited by IL-6.[30] In vitro, TN-C-stimulated DCs produced a high amount of IL-6 (Figure 5B and 5C), and then a blockade of IL-6 inhibits the TN-C-mediated Th17 polarization (Figure 5D). Taken together, TN-C influences the generation of pathogenic Th17 cells through its ability to promote IL-6 synthesis from DCs and forms an important link from innate to adaptive immunity. Moreover, IL-1 and granulocyte/macrophage colony-stimulating factor are known as factors promoting the generation and maintenance of Th17 cells.[55,56] Our results indicating that TN-C promoted IL-1 and granulocyte/macrophage colony-stimulating factor production by DCs (Figure 5B) might also explain the Th17 expansion in WT mice. Consistent with our data, there is evidence that TN-C plays a role in promoting T-cell activation[14] and polarization.[12,57]

Finally, we confirmed that the interaction of TN-C and DCs depended on TLR4-mediated signaling. Originally, TLR4 was shown to play a critical role in the recognition of LPS and subsequent signal transduction.[32] However, recent

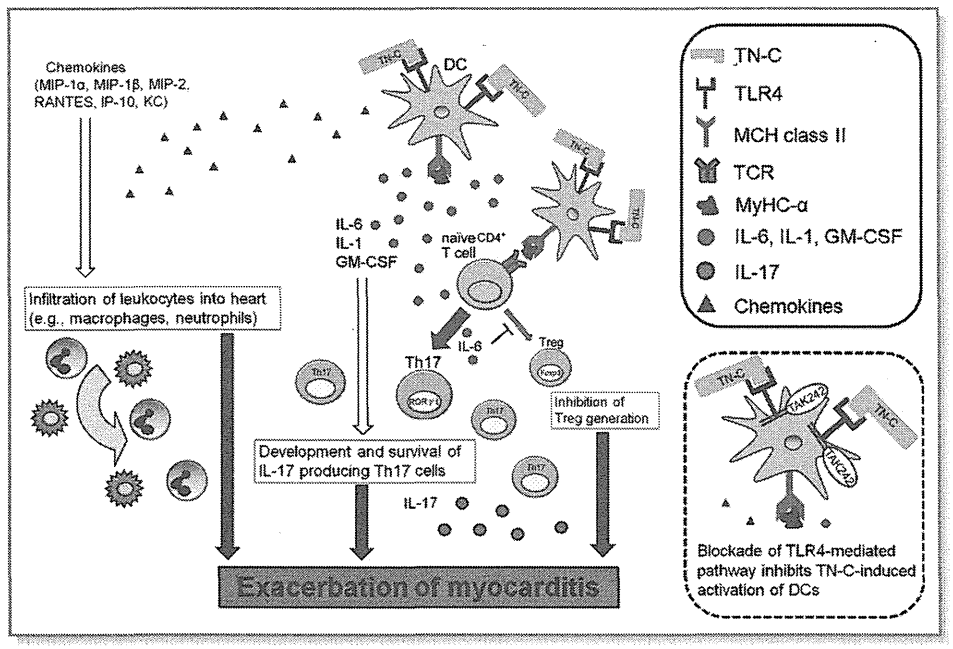

Figure 9. Schematic illustration showing how tenascin-C (TN-C)-stimulated dendritic cells (DCs) induce myocarditis. TN-C aggravates myocardial inflammation by stimulation of myosin-loaded DCs via Toll-like receptor (TLR)-4-mediated signaling. DCs stimulated by TN-C produce cytokines and growth factors (IL-6, IL-1, and GM-CSF) that contribute to the generation of cardiac myosin epitope peptide (MyHC)-α-specific Th17 cells. Chemokines secreted by TN-C-stimulated DCs help to accumulate inflammatory cells into the inflamed heart. GM-CSF indicates granulocyte/macrophage colony-stimulating factor; IL, interleukin; IP, IFN-γ-induced protein; KC, keratinocyte chemoattractant; MHC, major histocompatibility complex; MIP, macrophage inflammatory protein; RANTES, regulated on activation, normal T-cell expressed and secreted; TCR, T-cell receptor.

DOI: 10.1161/JAHA.114.001052

studies have indicated that TLR4 also plays a critical role in inflammatory responses to endogenous triggers.[58] Moreover, it was reported that self-antigen-loaded DCs activated via TLR4 stimulation by endogenous ligands generated by tissue damage is sufficient for the initiation of an autoimmune response in genetically susceptible individuals.[59] Thus, the TLR4 signaling pathway is an important mediator of autoimmune reactions that cause inflammation-induced injury in the myocardium. In the present study, the lack of TLR4-mediated signaling canceled the effects of TN-C on DCs to produce cytokines or chemokines and IL-17 secretion from Th17 cells (Figure 6). TLR4 signaling is composed of 2 distinct pathways. One is a MyD88-dependent pathway that is critical to the induction of inflammatory cytokines including IL-1β, IL-6, and IL-12p40.[32,60] The other is a Toll/IL-1R domain-containing adapter inducing IFN-β (TRIF)-dependent pathway that regulates the enhancement of DC maturation and induction of IP-10.[32,60] TAK242, a selective TLR4 signal transduction inhibitor, interferes with the interaction between TLR4 and the adaptor molecules of both pathways.[61] Therefore, TAK242 could reduce IL-1β, IL-6, IL-12p40, and IP-10 secretion from DCs at the same level of TLR4 deficiency generated by the inhibition of both the MyD88- and TRIF-dependent pathways (Figure 6A and 6B). Regarding the concern that a deficiency of TLR4 and its downstream signaling in TNKO mice may have an effect on the protection from myocarditis, we found no differences in TLR4 expression and NF-κB activation between WT and TNKO mice (Figure 7). Lastly, we confirmed that a TLR4 deficiency canceled the effect of TN-C in promoting DC-mediated myocarditis and attenuated the inflammation in vivo (Figure 8). This result provides direct evidence that blocking the TLR4-mediated pathway is effective in inhibiting TN-C-mediated myocardial inflammation.

A growing body of evidence suggests that TN-C is highly expressed in various inflammatory lesions of the heart, such as the Coxsackie virus B3–induced viral myocarditis model, another mouse model of myocarditis,[62,63] or the angiotensin II–induced hypertensive inflammation/fibrosis heart model,[19,64] and it may modulate the immune system during tissue remodeling. Indeed, deletion of TN-C reduces ventricular remodeling after myocardial infarction, suggesting that TN-C may play an important role in the pathology of remodeling by modulating inflammation.[65]

In conclusion, TN-C plays crucial roles in Th17 differentiation through the induction of IL-6 from DCs as a critical event for the initiation of EAM. Our proposed mechanism of a TN-C-mediated progression of myocardial inflammation is illustrated in Figure 9. Our data provide the first evidence that TN-C activation of DCs via the common receptor, TLR4, is critical for the expansion of EAM and provides new insight into a possible therapeutic target for autoimmune myocarditis.

Acknowledgments

The authors thank Y. Tsujimura for critical discussions and M. Hara and M. Namikata for providing technical assistance.

Sources of Funding

This work was supported by Health Science Research grants from the Ministry of Health, Labor and Welfare of Japan and the Ministry of Education, Culture, Sports, Science and Technology of Japan to Tajiri (No. 25860581), and a research grant for intractable diseases from the Ministry of Health, Labor and Welfare of Japan and The Okasan-Kato Foundation to Imanaka-Yoshida.

Disclosures

None.

References

1. Cihakova D, Rose NR. Pathogenesis of myocarditis and dilated cardiomyopathy. *Adv Immunol.* 2008;99:95–114.
2. Kindermann I, Barth C, Mahfoud F, Ukena C, Lenski M, Yilmaz A, Klingel K, Kandolf R, Sechtem U, Cooper LT, Bohm M. Update on myocarditis. *J Am Coll Cardiol.* 2012;59:779–792.
3. Eriksson U, Penninger JM. Autoimmune heart failure: new understandings of pathogenesis. *Int J Biochem Cell Biol.* 2005;37:27–32.
4. Fairweather D, Kaya Z, Shellam GR, Lawson CM, Rose NR. From infection to autoimmunity. *J Autoimmun.* 2001;16:175–186.
5. Eriksson U, Ricci R, Hunziker L, Kurrer MO, Oudit GY, Watts TH, Sonderegger I, Bachmaier K, Kopf M, Penninger JM. Dendritic cell-induced autoimmune heart failure requires cooperation between adaptive and innate immunity. *Nat Med.* 2003;9:1484–1490.
6. Joffre O, Nolte MA, Spörri R, Reis e Sousa C. Inflammatory signals in dendritic cell activation and the induction of adaptive immunity. *Immunol Rev.* 2009;227:234–247.
7. Midwood KS, Hussenet T, Langlois B, Orend G. Advances in tenascin-C biology. *Cell Mol Life Sci.* 2011;68:3175–3199.
8. Lund SA, Giachelli CM, Scatena M. The role of osteopontin in inflammatory processes. *J Cell Commun Signal.* 2009;3:311–322.
9. Li S, Yu Y, Koehn CD, Zhang Z, Su K. Galectins in the pathogenesis of rheumatoid arthritis. *J Clin Cell Immunol.* 2013;4:1000164.
10. Chiquet-Ehrismann R, Orend G, Chiquet M, Tucker RP, Midwood KS. Tenascins in stem cell niches. *Matrix Biol.* 2014; doi:10.1016/j.matbio.2014.01.007. [Epub ahead of print].
11. El-Karef A, Yoshida T, Gabazza EC, Nishioka T, Inada H, Sakakura T, Imanaka-Yoshida K. Deficiency of tenascin-C attenuates liver fibrosis in immune-mediated chronic hepatitis in mice. *J Pathol.* 2007;211:86–94.
12. Kanayama M, Morimoto J, Matsui Y, Ikesue M, Danzaki K, Kurotaki D, Ito K, Yoshida T, Uede T. α9β1 integrin-mediated signaling serves as an intrinsic regulator of pathogenic Th17 cell generation. *J Immunol.* 2011;187:5851–5864.
13. Midwood K, Sacre S, Piccinini AM, Inglis J, Trebaul A, Chan E, Drexler S, Sofat N, Kashiwagi M, Orend G, Brennan F, Foxwell B. Tenascin-C is an endogenous activator of Toll-like receptor 4 that is essential for maintaining inflammation in arthritic joint disease. *Nat Med.* 2009;15:774–780.
14. Nakahara H, Gabazza EC, Fujimoto H, Nishii Y, D'Alessandro-Gabazza CN, Bruno NE, Takagi T, Hayashi T, Maruyama J, Maruyama K, Imanaka-Yoshida K, Suzuki K, Yoshida T, Adachi Y, Taguchi O. Deficiency of tenascin C attenuates allergen-induced bronchial asthma in the mouse. *Eur J Immunol.* 2006;36:3334–3345.
15. Imanaka-Yoshida K, Hiroe M, Yasutomi Y, Toyozaki T, Tsuchiya T, Noda N, Maki T, Nishikawa T, Sakakura T, Yoshida T. Tenascin-C is a useful marker for disease activity in myocarditis. *J Pathol.* 2002;197:388–394.
16. Kanayama M, Kurotaki D, Morimoto J, Asano T, Matsui Y, Nakayama Y, Saito Y, Ito K, Kimura C, Iwasaki N, Suzuki K, Harada T, Li HM, Uehara J, Miyazaki T,

Minami A, Kon S, Uede T. α9 integrin and its ligands constitute critical joint microenvironments for development of autoimmune arthritis. *J Immunol*. 2009;182:8015–8025.

17. Imanaka-Yoshida K. Tenascin-C in cardiovascular tissue remodeling: from development to inflammation and repair. *Circ J*. 2012;76:2513–2520.
18. Sato A, Aonuma K, Imanaka-Yoshida K, Yoshida T, Isobe M, Kawase D, Kinoshita N, Yazaki Y, Hiroe M. Serum tenascin-C might be a novel predictor of left ventricular remodeling and prognosis after acute myocardial infarction. *J Am Coll Cardiol*. 2006;47:2319–2325.
19. Nishioka T, Suzuki M, Onishi K, Takakura N, Inada H, Yoshida T, Hiroe M, Imanaka-Yoshida K. Eplerenone attenuates myocardial fibrosis in the angiotensin II-induced hypertensive mouse: involvement of tenascin-C induced by aldosterone-mediated inflammation. *J Cardiovasc Pharmacol*. 2007;49:261–268.
20. Sato M, Toyozaki T, Odaka K, Uehara T, Arano Y, Hasegawa H, Yoshida K, Imanaka-Yoshida K, Yoshida T, Hiroe M, Tadokoro H, Irie T, Tanada S, Komuro I. Detection of experimental autoimmune myocarditis in rats by 111 in monoclonal antibody specific for tenascin-C. *Circulation*. 2002;106:1397–1402.
21. Tsukada B, Terasaki F, Shimomura H, Otsuka K, Otsuka K, Katashima T, Fujita S, Imanaka-Yoshida K, Yoshida T, Hiroe M, Kitaura Y. High prevalence of chronic myocarditis in dilated cardiomyopathy referred for left ventriculoplasty: expression of tenascin C as a possible marker for inflammation. *Hum Pathol*. 2009;40:1015–1022.
22. Saga Y, Yagi T, Ikawa Y, Sakakura T, Aizawa S. Mice develop normally without tenascin. *Genes Dev*. 1992;6:1821–1831.
23. Tajiri K, Imanaka-Yoshida K, Matsubara A, Tsujimura Y, Hiroe M, Naka T, Shimojo N, Sakai S, Aonuma K, Yasutomi Y. Suppressor of cytokine signaling 1 DNA administration inhibits inflammatory and pathogenic responses in autoimmune myocarditis. *J Immunol*. 2012;189:2043–2053.
24. Lutz MB, Kukutsch N, Ogilvie AL, Rossner S, Koch F, Romani N, Schuler G. An advanced culture method for generating large quantities of highly pure dendritic cells from mouse bone marrow. *J Immunol Methods*. 1999; 223:77–92.
25. Kalembey I, Yoshida T, Iriyama K, Sakakura T. Analysis of tenascin mRNA expression in the murine mammary gland from embryogenesis to carcinogenesis: an in situ hybridization study. *Int J Dev Biol*. 1997;41:569–573.
26. Imanaka-Yoshida K, Hiroe M, Nishikawa T, Ishiyama S, Shimojo T, Ohta Y, Sakakura T, Yoshida T. Tenascin-C modulates adhesion of cardiomyocytes to extracellular matrix during tissue remodeling after myocardial infarction. *Lab Invest*. 2001;81:1015–1024.
27. Pinet É. Fabry-Pérot fiber-optic sensors for physical parameters measurement in challenging conditions. *J Sens*. 2009;2009:1–9.
28. Valaperti A, Marty RR, Kania G, Germano D, Mauermann N, Dirnhofer S, Leimenstoll B, Blyszczuk P, Dong C, Mueller C, Hunziker L, Eriksson U. Cd11b$^+$ monocytes abrogate Th17 CD4$^+$ T cell-mediated experimental autoimmune myocarditis. *J Immunol*. 2008;180:2686–2695.
29. Twerenbold R, Jaffe A, Reichlin T, Reiter M, Mueller C. High-sensitive troponin T measurements: what do we gain and what are the challenges? *Eur Heart J*. 2012;33:579–586.
30. Bettelli E, Carrier Y, Gao W, Korn T, Strom TB, Oukka M, Weiner HL, Kuchroo VK. Reciprocal developmental pathways for the generation of pathogenic effector Th17 and regulatory T cells. *Nature*. 2006;441:235–238.
31. Orend G. Potential oncogenic action of tenascin-C in tumorigenesis. *Int J Biochem Cell Biol*. 2005;37:1066–1083.
32. Kawai T, Takeuchi O, Fujita T, Inoue J, Muhlradt PF, Sato S, Hoshino K, Akira S. Lipopolysaccharide stimulates the MyD88-independent pathway and results in activation of IFN-regulatory factor 3 and the expression of a subset of lipopolysaccharide-inducible genes. *J Immunol*. 2001;167:5887–5894.
33. Fujimoto N, Onishi K, Sato A, Terasaki F, Tsukada B, Nozato T, Yamada T, Imanaka-Yoshida K, Yoshida T, Ito M, Hiroe M. Incremental prognostic values of serum tenascin-C levels with blood B-type natriuretic peptide testing at discharge in patients with dilated cardiomyopathy and decompensated heart failure. *J Card Fail*. 2009;15:898–905.
34. Waldner H. The role of innate immune responses in autoimmune disease development. *Autoimmun Rev*. 2009;8:400–404.
35. Renkl AC, Wussler J, Ahrens T, Thoma K, Kon S, Uede T, Martin SF, Simon JC, Weiss JM. Osteopontin functionally activates dendritic cells and induces their differentiation toward a Th1-polarizing phenotype. *Blood*. 2005; 106:946–955.
36. Schulz G, Renkl AC, Seier A, Liaw L, Weiss JM. Regulated osteopontin expression by dendritic cells decisively affects their migratory capacity. *J Invest Dermatol*. 2008;128:2541–2544.
37. Fulcher JA, Chang MH, Wang S, Almazan T, Hashimi ST, Eriksson AU, Wen X, Pang M, Baum LG, Singh RR, Lee B. Galectin-1 co-clusters CD43/CD45 on dendritic cells and induces cell activation and migration through Syk and protein kinase c signaling. *J Biol Chem*. 2009;284:26860–26870.
38. Fulcher JA, Hashimi ST, Levroney EL, Pang M, Gurney KB, Baum LG, Lee B. Galectin-1-matured human monocyte-derived dendritic cells have enhanced migration through extracellular matrix. *J Immunol*. 2006;177:216–226.
39. Levroney EL, Aguilar HC, Fulcher JA, Kohatsu L, Pace KE, Pang M, Gurney KB, Baum LG, Lee B. Novel innate immune functions for galectin-1: galectin-1 inhibits cell fusion by Nipah virus envelope glycoproteins and augments dendritic cell secretion of proinflammatory cytokines. *J Immunol*. 2005;175:413–420.
40. Eriksson U, Kurrer MO, Sebald W, Brombacher F, Kopf M. Dual role of the IL-12/IFN-gamma axis in the development of autoimmune myocarditis: induction by IL-12 and protection by IFN-gamma. *J Immunol*. 2001;167:5464–5469.
41. Eriksson U, Kurrer MO, Sonderegger I, Iezzi G, Tafuri A, Hunziker L, Suzuki S, Bachmaier K, Bingisser RM, Penninger JM, Kopf M. Activation of dendritic cells through the interleukin 1 receptor 1 is critical for the induction of autoimmune myocarditis. *J Exp Med*. 2003;197:323–331.
42. Eriksson U, Kurrer MO, Schmitz N, Marsch SC, Fontana A, Eugster HP, Kopf M. Interleukin-6-deficient mice resist development of autoimmune myocarditis associated with impaired upregulation of complement C3. *Circulation*. 2003;107:320–325.
43. Göser S, Ottl R, Brodner A, Dengler TJ, Torzewski J, Egashira K, Rose NR, Katus HA, Kaya Z. Critical role for monocyte chemoattractant protein-1 and macrophage inflammatory protein-1alpha in induction of experimental autoimmune myocarditis and effective anti-monocyte chemoattractant protein-1 gene therapy. *Circulation*. 2005;112:3400–3407.
44. Leib C, Göser S, Luthje D, Öttl R, Tretter T, Lasitschka F, Zittrich S, Pfitzer G, Katus HA, Kaya Z. Role of the cholinergic antiinflammatory pathway in murine autoimmune myocarditis. *Circ Res*. 2011;109:130–140.
45. Kishimoto C, Kawamata H, Sakai S, Shinohara H, Ochiai H. Enhanced production of macrophage inflammatory protein 2 (MIP-2) by in vitro and in vivo infections with encephalomyocarditis virus and modulation of myocarditis with an antibody against MIP-2. *J Virol*. 2001;75:1294–1300.
46. Ritzman AM, Hughes-Hanks JM, Blaho VA, Wax LE, Mitchell WJ, Brown CR. The chemokine receptor CXCR2 ligand KC (CXCL1) mediates neutrophil recruitment and is critical for development of experimental Lyme arthritis and carditis. *Infect Immun*. 2010;78:4593–4600.
47. Yue Y, Gui J, Ai W, Xu W, Xiong S. Direct gene transfer with IP-10 mutant ameliorates mouse CVB3-induced myocarditis by blunting Th1 immune responses. *PLoS One*. 2011;6:e18186.
48. Zimmermann O, Kochs M, Zwaka TP, Kaya Z, Lepper PM, Bienek-Ziolkowski M, Hoher M, Hombach V, Torzewski J. Myocardial biopsy based classification and treatment in patients with dilated cardiomyopathy. *Int J Cardiol*. 2005;104:92–100.
49. Goh FG, Piccinini AM, Krausgruber T, Udalova IA, Midwood KS. Transcriptional regulation of the endogenous danger signal tenascin-C: a novel autocrine loop in inflammation. *J Immunol*. 2010;184:2655–2662.
50. Morimoto S, Imanaka-Yoshida K, Hiramitsu S, Kato S, Ohtsuki M, Uemura A, Kato Y, Nishikawa T, Toyozaki T, Hishida H, Yoshida T, Hiroe M. Diagnostic utility of tenascin-C for evaluation of the activity of human acute myocarditis. *J Pathol*. 2005;205:460–467.
51. Sonderegger I, Röhn TA, Kurrer MO, Iezzi G, Zou Y, Kastelein RA, Bachmann MF, Kopf M. Neutralization of IL-17 by active vaccination inhibits IL-23-dependent autoimmune myocarditis. *Eur J Immunol*. 2006;36:2849–2856.
52. Sakaguchi S. Naturally arising CD4$^+$ regulatory t cells for immunologic self-tolerance and negative control of immune responses. *Annu Rev Immunol*. 2004;22:531–562.
53. Cruz-Adalia A, Jiménez-Borreguero LJ, Ramírez-Huesca M, Chico-Calero I, Barreiro O, López-Conesa E, Fresno M, Sánchez-Madrid F, Martín P. CD69 limits the severity of cardiomyopathy after autoimmune myocarditis. *Circulation*. 2010;122:1396–1404.
54. Yamashita T, Iwakura T, Matsui K, Kawaguchi H, Obana M, Hayama A, Maeda M, Izumi Y, Komuro I, Ohsugi Y, Fujimoto M, Naka T, Kishimoto T, Nakayama H, Fujio Y. IL-6-mediated Th17 differentiation through RORγt is essential for the initiation of experimental autoimmune myocarditis. *Cardiovasc Res*. 2011;91:640–648.
55. Chung Y, Chang SH, Martinez GJ, Yang XO, Nurieva R, Kang HS, Ma L, Watowich SS, Jetten AM, Tian Q, Dong C. Critical regulation of early Th17 cell differentiation by interleukin-1 signaling. *Immunity*. 2009;30:576–587.
56. Sonderegger I, Iezzi G, Maier R, Schmitz N, Kurrer M, Kopf M. GM-CSF mediates autoimmunity by enhancing IL-6-dependent Th17 cell development and survival. *J Exp Med*. 2008;205:2281–2294.
57. Ruhmann M, Piccinini AM, Kong PL, Midwood KS. Endogenous activation of adaptive immunity: tenascin-C drives interleukin-17 synthesis in murine arthritic joint disease. *Arthritis Rheum*. 2012;64:2179–2190.

58. Liu Y, Yin H, Zhao M, Lu Q. TLR2 and TLR4 in autoimmune diseases: a comprehensive review. *Clin Rev Allergy Immunol.* 2013; doi: 10.1007/s12016-013-8402-y [Epub ahead of print].

59. Tsan MF, Gao B. Endogenous ligands of Toll-like receptors. *J Leukoc Biol.* 2004;76:514–519.

60. Kaisho T, Takeuchi O, Kawai T, Hoshino K, Akira S. Endotoxin-induced maturation of MyD88-deficient dendritic cells. *J Immunol.* 2001;166:5688–5694.

61. Matsunaga N, Tsuchimori N, Matsumoto T, Ii M. TAK-242 (resatorvid), a small-molecule inhibitor of Toll-like receptor (TLR) 4 signaling, binds selectively to TLR4 and interferes with interactions between TLR4 and its adaptor molecules. *Mol Pharmacol.* 2011;79:34–41.

62. Ruppert V, Meyer T, Pankuweit S, Jonsdottir T, Maisch B. Activation of STAT1 transcription factor precedes up-regulation of coxsackievirus-adenovirus receptor during viral myocarditis. *Cardiovasc Pathol.* 2008;17:81–92.

63. Leipner C, Grün K, Müller A, Buchdunger E, Borsi L, Kosmehl H, Berndt A, Janik T, Uecker A, Kiehntopf M, Böhmer FD. Imatinib mesylate attenuates fibrosis in coxsackievirus B3-induced chronic myocarditis. *Cardiovasc Res.* 2008;79:118–126.

64. Fujita S, Shimojo N, Terasaki F, Otsuka K, Hosotani N, Kohda Y, Tanaka T, Nishioka T, Yoshida T, Hiroe M, Kitaura Y, Ishizaka N, Imanaka-Yoshida K. Atrial natriuretic peptide exerts protective action against angiotensin II-induced cardiac remodeling by attenuating inflammation via endothelin-1/endothelin receptor A cascade. *Heart Vessels.* 2013;28:646–657.

65. Nishioka T, Onishi K, Shimojo N, Nagano Y, Matsusaka H, Ikeuchi M, Ide T, Tsutsui H, Hiroe M, Yoshida T, Imanaka-Yoshida K. Tenascin-C may aggravate left ventricular remodeling and function after myocardial infarction in mice. *Am J Physiol.* 2010;298:H1072–H1078.

Antiviral Research 113 (2015) 93–102

Contents lists available at ScienceDirect

Antiviral Research

journal homepage: www.elsevier.com/locate/antiviral

Inhibitory effects of Pycnogenol® on hepatitis C virus replication

Sayeh Ezzikouri [a,b,c,1], Tomohiro Nishimura [d,1], Michinori Kohara [e], Soumaya Benjelloun [a], Yoichiro Kino [d], Kazuaki Inoue [f], Akira Matsumori [g], Kyoko Tsukiyama-Kohara [b,c,*]

[a] Virology Unit, Viral Hepatitis Laboratory, Pasteur Institute of Morocco, Casablanca, Morocco
[b] Transboundary Animal Diseases Centre, Joint Faculty of Veterinary Medicine, Kagoshima University, Kagoshima, Japan
[c] Laboratory of Animal Hygiene, Joint Faculty of Veterinary Medicine, Kagoshima University, Kagoshima, Japan
[d] Chemo-Sero Research Institute, Kikuchi Research Center, Kumamoto, Japan
[e] Department of Microbiology and Cell Biology, Tokyo Metropolitan Institute of Medical Science, Tokyo, Japan
[f] Division of Gastroenterology, Showa University, Fujigaoka Hospital, Kanagawa, Japan
[g] Tokyo Medical University, Tokyo, Japan

ARTICLE INFO

Article history:
Received 30 June 2014
Revised 24 October 2014
Accepted 31 October 2014
Available online 20 November 2014

Keywords:
Natural product
Resistant
ROS
Antioxidant
Replication

ABSTRACT

Chronic hepatitis C virus (HCV) infection increases the risk of liver cirrhosis and hepatocellular carcinoma. In the last decade, the current standard HCV treatment, pegylated interferon and ribavirin, have limited efficacy and significant side effects. Novel direct acting antivirals show promise, but escape mutants are expected, along with potential side effects. Pycnogenol®, a French maritime pine extract, has been reported to have antioxidant and antiviral effects. Here, we evaluated the effect of Pycnogenol® on HCV replication.

Wild-type and protease inhibitor (VX-950; telaprevir)-resistant HCV replicon cells were treated with Pycnogenol®, Pycnogenol® and interferon-alpha, and ribavirin and telaprevir. Pycnogenol® effects on replication were also evaluated in HCV-infected chimeric mice.

Pycnogenol® treatment showed antiviral effects without cytotoxicity at doses up to 50 μg/mL. Pycnogenol® in combination with interferon-alpha or ribavirin showed synergistic effects. Moreover, Pycnogenol® inhibited HCV replication in telaprevir-resistant replicon cells; telaprevir and Pycnogenol® acted additively to reduce HCV RNA levels in wild-type HCV replicon cells without significantly increasing cytotoxicity. Pycnogenol® antiviral activity was higher than its components procyanidin and taxifolin. Further, treatment of infected chimeric mice with Pycnogenol® suppressed HCV replication and showed a synergistic effect with interferon-alpha. In addition, Pycnogenol® treatment resulted in dose-dependent reduction of reactive oxygen species in HCV replicon cell lines.

Pycnogenol® is a natural product that may be used to improve the efficacy of the current standard antiviral agents and even to eliminate resistant HCV mutants.

1. Introduction

Approximately 130–170 million people are chronically infected with HCV, leading to 54,000 deaths and 955,000 disability-adjusted life-years associated with acute HCV infection (Mohd Hanafiah et al., 2013). Chronic hepatitis C can lead to a large spectrum of diseases, including steatosis, fibrosis, cirrhosis, and hepatocellular carcinoma (Perz and Alter, 2006). To date, no protective vaccine is available for HCV infection; over the last decade, therapy has consisted of a 24–48-week course of peginterferon-alpha-2a (PEG-IFN-alpha-2a) or peginterferon-alpha-2b (PEG-IFN-alpha-2b) in combination with the guanosine analogue, ribavirin (RBV). The therapy leads to sustained virologic response (SVR) in 42–52%, 65–85%, and 76–82% of individuals infected with HCV genotype 1; 4, 5, or 6; and 2 or 3, respectively (Antaki et al., 2010; Hoofnagle and Seeff, 2006). The recently approved non-structural

Abbreviations: CC_{50}, 50% cytotoxic concentration; CI, combination index; DAA, direct acting antivirals; EC_{50}, 50% effective concentration; HCV, hepatitis C virus; IC_{50}, 50% inhibitory concentration; IRES, internal ribosome entry site; NS, non-structural protein; NF-kappa B, nuclear factor-kappa B; PC, procyanidin; PEG-IFN-alpha-2a, pegylated interferon-alpha-2a; PEG-IFN-alpha-2b, pegylated interferon-alpha-2b; RBV, ribavirin; PYC, Pycnogenol®; qRT-PCR, quantitative real-time reverse transcription polymerase chain reaction; ROS, reactive oxygen species; SI, selectivity index.

* Corresponding author at: Transboundary Animal Diseases Centre & Department of Animal Hygiene, Joint Faculty of Veterinary Medicine, Kagoshima University, 1-21-24 Korimoto, Kagoshima-city 890-0065, Japan. Tel./fax: +81 99 285 3589.

E-mail addresses: sayeh.ezzikouri@pasteur.ma (S. Ezzikouri), kkohara@vet.kagoshima-u.ac.jp (K. Tsukiyama-Kohara).

[1] These authors contributed equally to the study.

http://dx.doi.org/10.1016/j.antiviral.2014.10.017
0166-3542/

protein (NS) 3/4A protease inhibitors (PIs) boceprevir (approved by the FDA on May 13, 2011) and telaprevir (approved by the FDA on May 23, 2011), used in combination with PEG-IFN-alpha and RBV for HCV genotype 1 infections, have increased cure rates to approximately 70% (Bacon et al., 2011; Jacobson et al., 2011; Poordad et al., 2011). However, these triple-therapy regimens may result in unfavourable side effects and emergence of drug-resistant HCV (Bacon et al., 2011; Jacobson et al., 2011; Poordad et al., 2011), which may reduce virus susceptibility and applicability of current HCV triple therapies (Ozeki et al., 2011). Recently, two more effective compounds have been approved for HCV treatment: the protease inhibitor simeprevir (approved by the FDA in November, 2013) and the nucleotide polymerase inhibitor sofosbuvir (approved by the FDA on December 6, 2013). Among patients infected with HCV, less than 10% are treated and cured, and the major challenge in controlling HCV infections is the identification of those already infected, most of whom are situated in the poorest regions of the world (Thomas, 2013), and to find the most effective, tolerable and affordable direct acting antivirals (DAA) combination that can cure people in the shortest period (Poveda et al., 2014). In the NEUTRINO phase III trial of treatment-naive patients, 12 weeks of triple combination therapy with sofosbuvir (400 mg) once daily resulted in SVR rates of 89% in patients with HCV genotype 1 (92% for subtype 1a and 82% for subtype 1b), and 96% in patients with genotype 4 (Lawitz et al., 2013). Moreover, in the FISSION trial of HCV-2/3 treatment-naive patients receiving sofosbuvir/RBV for 12 weeks, 95% of patients with genotype 2 and 56% of patients with genotype 3 achieved an SVR (Lawitz et al., 2013). In addition, most DAA agents are characterised by a low genetic barrier to the development of resistance, except sofosbuvir, which showed a very high resistance barrier. This is the reason most current DAA-based therapies under evaluation must be co-administered with either PEG-IFN-alpha and ribavirin or different compounds belonging to different DAA classes (Poveda et al., 2014).

Pycnogenol® (PYC; trademark of Horphag Research, Geneva, Switzerland) is a French maritime pine extract produced from the outer bark of *Pinus pinaster* ssp. *atlantica*, and is generally considered safe for human use (American Botanical Council, 2010). The main PYC constituents are procyanidins (68.4%), taxifolin (21.87%), ferulic acid (3.70%), catechin (2.53%), and caffeic acid (3.51%) (Lee et al., 2010). PYC has been reported to have antioxidative and anti-inflammatory effects, and to reduce cardiovascular risk factors associated with type 2 diabetes (Maimoona et al., 2011; Zibadi et al., 2008). A recent report suggests that PYC can inhibit encephalomyocarditis virus replication in the mouse heart by suppressing expression of proinflammatory cytokines, and genes related to cardiac remodelling and mast cells (Matsumori et al., 2007). PYC has also been reported to inhibit binding of human immunodeficiency virus type-1 to host cells, and to cause other significant changes, including increased expression of manganese superoxide dismutase (Feng et al., 2008).

HCV gene expression elevates reactive oxygen species (ROS) levels via calcium signalling. In addition, HCV Core, NS3, and NS5A proteins have all been shown to induce oxidative stress (Choi et al., 2004). The reported link between HCV and oxidative stress makes this pathway a promising anti-HCV therapeutic strategy. To date, however, the effect of PYC on HCV infection has not been investigated. This study evaluated the inhibitory effects of Pycnogenol® on HCV replication *in vitro* and *in vivo*.

2. Materials and methods

2.1. Cell culture and reagents

Genotype 1b HCV subgenomic replicon cell lines, R6FLR-N (R6, genotype 1b, strain N) (Watanabe et al., 2006), FLR3-1 (genotype 1b, Con-1) (Sakamoto et al., 2005) and Rep JFH Luc3-13 genotype 2a (Takano et al., 2011), strain JFH-1 (Wakita et al., 2005) (Supplementary Fig. 1) were cultured at 37 °C (5% CO_2) in Dulbecco's modified Eagle medium-GlutaMAX-I (DMEM-GlutaMAX-I; Invitrogen, Carlsbad, CA, USA) containing 10% foetal bovine serum and 0.5 mg/mL G418 (Invitrogen, Carlsbad, CA, USA) (Sakamoto et al., 2005; Watanabe et al., 2006). The JFH-1/K4 cell line, which comprises HuH-7 cells persistently infected with the HCV JFH-1 strain, was maintained in DMEM with 10% FCS (Takano et al., 2011).

PYC was supplied by Horphag Research Co., Pegylated IFN-alpha-2a was obtained from Chugai Pharmaceutical Co., Japan.

2.2. HCV replicon cell reporter assay

Cells were seeded into 96-well plates (5×10^3/well). After incubation for 24 h at 37 °C (5% CO_2), the medium was removed and replaced with growth medium containing serial dilutions of PYC, IFN-alpha, RBV, telaprevir or simeprevir (Janssen Pharma Co., Tokyo, Japan). After 72 h, luciferase activity was measured using the Bright-Glo luciferase assay kit (Promega, Madison, WI). Measurements were made in triplicate using an AccuFLEX Lumi 400 luminometer (Aloka, Tokyo, Japan), and the results expressed as the average percentage of the control.

2.3. Generation of telaprevir-resistant replicon cell lines and analysis

Telaprevir-resistant R6FLR-N subgenomic replicon cell lines were established as described previously (Katsume et al., 2013). Briefly, wild-type R6FLR-N replicon cells were seeded in 10-cm dishes in the presence of 0.5 mg/mL G418 and treated with telaprevir. The cells were incubated for 51 days with no-compound control or telaprevir (1.8 μM and 2.7 μM serially diluted in media). Fresh media and telaprevir were added every 3 days. Most cells incubated with 2.7 μM telaprevir died; however, after 3 weeks small colonies started to appear and were expanded for 4 weeks. Deep sequencing was performed as described previously (Katsume et al., 2013) and revealed a mutation profile in NS3 (V36A, T54V and A156T) and NS5A (Q181H, P223S and S417P) which confer resistance to telaprevir. Resistant replicon cells were seeded at 5×10^3/well. After incubation for 24 h at 37 °C (5% CO_2), culture medium was removed and replaced with growth medium containing serial dilutions of PYC or telaprevir alone or in combination. After 72 h, luciferase activity was determined using the Bright-Glo luciferase assay kit (Promega, Madison, WI, USA). Measurements were made in duplicate using a GloMax-Multi detection system (Promega, Madison, WI, USA). Cytotoxicity was measured using WST-8 cell counting kit (Dojindo, Kumamoto, Japan). Western blot analysis was performed, as described previously (Nishimura et al., 2009). Briefly, HCV replicon cells (2×10^5) were grown in a 60-mm cell culture dish. After 24 h, cells were treated with PYC for 72 h. Cells were collected and lysed with radioimmunoprecipitation buffer (1% sodium dodecyl sulphate, 0.5% Nonidet P-40, 150 mmol NaCl, 0.5 mmol ethylenediaminetetraacetic acid, 1 mmol dithiothreitol, and 10 mmol Tris, pH 7.4). Total protein (30 μg) was electrophoresed on a 12% sodium dodecyl sulphate–polyacrylamide gel and transferred to a polyvinylidene difluoride membrane (Immobilon-P; Millipore, Billerica, MA, USA). HCV NS3 and NS5B proteins were detected using rabbit NS3 (R212) polyclonal antibody or anti-NS5B (5B14) monoclonal antibody. Beta-actin was detected using an actin monoclonal antibody (Sigma, St. Louis, MO, USA).

2.4. Quantitative real-time polymerase chain reaction

Quantification of HCV RNA was performed using real-time reverse transcription polymerase chain reaction (qRT-PCR) based